



DEGREE PROJECT IN CHEMICAL SCIENCE AND ENGINEERING,
SECOND CYCLE, 30 CREDITS
STOCKHOLM, SWEDEN 2016

Removal of hydrogen sulfide from an air stream using UV light

LORENZA GILARDI



KUNGLIGA TEKNISKA HÖGSKOLAN

POLITECNICO DI MILANO

MASTER'S THESIS

Removal of hydrogen sulfide from an air stream using UV light

Author:

Lorenza GILARDI

Examiner:

Prof. Klas ENGVALL

Supervisors:

Dr. Roberto LANZA

Dr. Mario GROSSO

Francesco MONTECCHIO

Monday 23rd November, 2015

Abstract

Volatile sulfur compounds are cause of concern because, when present in high concentrations, they constitute a danger for health because of their strong toxicity. Furthermore, for low concentrations, they are often cause of complaint, because of their low odor threshold. In this context, the purpose of this Thesis is to evaluate a new technology for the abatement of Sulfur-based malodorous compounds. The investigated technology consists in the use of Ozone generating low pressure UV mercury lamps, operating at room temperature. Hydrogen sulfide is often found in industrial processes, (e.g. WWTPs (Wastewater Treatment Plants), leather production, sewage treatment, garbage disposal,...). Moreover, it presents both a very high toxicity a low odor threshold. Thus, due to its high representativeness of the case, hydrogen sulfide was chosen as reference compound for the purposes of this project. In order to evaluate a wide range of cases, several experiments using different residence times, humidity contents and inlet concentrations of the pollutant were conducted. The obtained results show that this technology generally presents discrete conversion efficiencies, although not sufficient to be used as freestanding process. For this reason, a pretreatment is revealed to be necessary. The best conversion efficiency was obtained for low flow rates and high moisture content. At the end of the project, as side-study, a possible pre-treatment using an adsorbent bed constituted by granular ferric oxide was evaluated.

Contents

Acronyms	viii
1 Introduction	2
1.1 Objectives of the Study	4
2 Volatile sulfur compounds	5
2.1 Sources	5
2.2 Current treatment technologies for volatile sulfur compounds	7
3 Hydrogen sulfide removal mechanism in the photoreactor	13
4 Experimental planning	17
4.1 Main parameters	17
4.2 Preliminary tests: methodology	20
4.3 Tests with hydrogen sulfide: methodology	21
5 Experimental setup	22
5.1 System configuration	22
5.2 Instruments and devices	24
6 Results	33
6.1 Preliminary tests	33
6.2 Hydrogen sulfide tests	35
7 Conclusions	52

8	Future work	55
	Bibliography	58
A	Study of a pre-treatment	62
A.1	Description of the material	62
A.2	Main parameters	63
A.3	Methodology	64
A.4	System configuration: adsorption	64

List of Figures

2.1	Process scheme of gas scrubbing.[1]	7
2.2	Adsorption reactor configuration[1]	8
2.3	Incineration system configuration[1]	9
2.4	Biofiltration reactor configuration[1]	10
2.5	Bioscrubber reactor configuration[1]	11
3.1	Comparison of the ozone densities obtained from simulation and experiments under different humidity, O ₂ concentration, and flow conditions[2].	16
4.1	Sizes of the photoreactor	19
5.1	P&ID system scheme of oxidation using UV light producing ozone	23
5.2	Photo of the complete system	24
5.3	Humidification system	25
5.4	Photo of the glass ampoule containing the hygrometer probe	26
5.5	Drawing of the stainless steel body of the photoreactor obtained with the software Autodesk Inventor	27
5.6	Stainless steel photoreactor	27
5.7	Heraeus GPH150T5VH/4 lamp	28
5.8	Wavelength distribution of the mercury low pressure ozone generating lamp	28
5.9	Operating diagram of the PID sensor [3]	29
5.10	Simplified scheme of the system composed by a GC followed by a SCD [4]	31
5.11	Figure showing the typical appearance of a chromatogram sequence	31

6.1	Diagram showing the obtained calibration factor	34
6.2	Results of the tests conducted with different moisture grades	35
6.3	Diagram showing the relation between the chromatogram area and the concentration	36
6.4	Comparison between the degradation obtained with different residence times for a condition of 21% of RH (the lowest allowed in the laboratory)	37
6.5	Comparison between the degradation obtained with different flow rates for a condition of 40% of RH	38
6.6	Comparison between the degradation obtained with different residence times for a condition of 60% of RH	38
6.7	Comparison between the degradation obtained with different RH with a given constant residence time of 3.29 s	39
6.8	Comparison between the degradation obtained with different RH with a given constant residence time of 2.47 s	39
6.9	Comparison between the degradation obtained with different RH with a given constant residence time of 1.7 s	40
6.10	Comparison between the degradation obtained for different inlet concentrations, for all the tests conducted	41
6.11	Tridimensional visualization of the data obtained, showing the relation between conversion, flow rate (residence time), and humidity having 20 ppm as inlet concentration. Under the tridimensional graph, the corresponding contouring graph	43
6.12	Tridimensional visualization of the data obtained, showing the relation between average residual ozone, flow rate (residence time), and humidity. Under the tridimensional graph, the corresponding contouring graph	44
6.13	Tridimensional visualization of the data obtained, showing the relation between residual ozone in blank tests, flow rate (residence time), and humidity. Under the tridimensional graph, the corresponding contouring graph	45

6.14	Tridimensional visualization of the data obtained, showing the trend of two important parameters, residual ozone and conversion, in the graph area corresponding to high residence time (3.29 s)	46
6.15	Tridimensional visualization of the data obtained, showing the trend of two important parameters, residual ozone and conversion, in the graph area corresponding to low humidity	48
6.16	Tridimensional visualization of the data obtained, showing the trend of two important parameters, residual ozone and conversion, in the graph area corresponding to high humidity and low residence time	49
6.17	Tridimensional visualization of the data obtained, the difference computed between the ozone detected in the blank tests and the residual ozone in the tests with addition on hydrogen sulfide	50
6.18	CFD simulations (by Francesco Montecchio) showing the mixing inside the reactor. The the top one shows the mixing corresponding to 15 <i>l/min</i> . The bottom one shows the mixing corresponding to 30 <i>l/min</i>	51
A.1	Pore size distribution of the granular ferric hydroxide provided by HeGo [®] Biotec	63
A.2	System scheme of adsorption with Iron Hydroxide	64
A.3	Outlet concentration from the pre-treatment beds VS time.	65
[totoc]		

List of Tables

1.1	Human physiologic responses to exposure to hydrogen sulfide [5]	3
2.1	Malodorous sulfur compounds summarized characteristics	6
2.2	Advantages and disadvantages of the current technologies available for odour treatment caused by VOCs [6][1] [7] [8].	12
4.1	Relation between flow rates and residence time in the reactor.	18
6.1	Relation between flow rates and residence time in the reactor.	37
7.1	Conversion corresponding to different inlet concentration for a residence time of 1.7 s and different humidity contents	53
8.1	Typical values of malodorous gases in different industrial plants	57
[totoc]		

List of Abbreviations

AC	Activated Carbon
Bp	Boiling point
CFD	Computational Fluid Dynamics
EBCT	Empty Bed Contact Time
GC	Gas Chromatograph
OT	Odour Threshold
PID	Photo Ionization Detector
RH	Relative Humidity
SCD	Sulfur Chemiluminescence Detector
STEL	Short Term Exposure Time
TLV	Threshold Limit Value
UV	Ultra Violet
VOC	Volatile Organic Compound
VSCs	Volatile Sulfur Compounds
WWTPs	Wastewater Treatment Plants

Chapter 1

Introduction

The concern on the pollution caused by malodorous compounds is growing because not only they are dangerous for human health, both in terms of discomfort and of temporary or permanent damage, but also because of their environmental impact. In this context, volatile sulfur compounds (VSCs) are a current subject of interest because of their high toxicity, their low odour threshold and their high corrosive properties on several materials. For these reasons, several technologies and strategies were studied, in order to improve the efficiency of the abatement of these chemicals in the air stream. The most common malodorous compounds of interest, that several industrial activities have to face, are: hydrogen sulfide (H_2S), dimethyl sulfide (M_2S), dimethyl sulfide (Me_2S_2), methyl mercaptan (MeSh), carbon disulfide (CS_2) and carbonyl sulfide (COS)[7].

Among malodorous VSCs, hydrogen sulfide presents a position of relevance. It is characterized by a typical rotten-egg odour and it is one of the most common sulfur odorous compound, present in several industry fields. More than 70 types of industries are associated with emissions of H_2S [9], including, food production, artificial fiber synthesis, roofing, paper and pulp manufacture and sewage treatment. Moreover, hydrogen sulfide is particularly critical in term of toxicity. The toxicity of H_2S has a direct correlation with the concentration of exposure, affecting the respiratory, cardiovascular, and nervous systems [10]. Acute responses can be observed even for exposures to low concentrations (< 50 ppm). Table 2.2 shows the effects on human

health caused by the exposure of different concentration levels of Hydrogen Sulfide. As it is possible to see, the maximum concentration associated to the odour perception is under 100 ppm. The technologies that are currently available in the field of odour treatment and their main characteristics are described in section 2.2.

Table 1.1 – Human physiologic responses to exposure to hydrogen sulfide [5]

Concentration [ppm]	Effect on human health [–]
0.003 – 0.002	Odor threshold
3 – 10	Obvious unpleasant odor
20 – 30	Strong offensive odor (“rotten eggs”)
30	Sickening sweet odor
50	Conjunctival irritation
50 – 100	Irritation of respiratory tract
100 – 200	Loss of smell (olfactory fatigue)
150 – 200	Olfactory paralysis
250 – 500	Pulmonary edema
500	Anxiety, headache, ataxia, dizziness, stimulation of respiration, amnesia, unconsciousness (“knockdown”)
500 – 1000	Respiratory paralysis leading to death, immediate collapse, neural paralysis, cardiac arrhythmias, death

1.1 Objectives of the Study

The aim of this study is to test the efficiency of a new technology in the field of the waste gases purification. The expectation is to be more energy efficient, if compared with the existing ones, since UV technology operates at room temperature and doesn't need fuel.

This goal was pursued by focusing mainly on the process temperature. The use of UV technology involves, indeed, the possibility to conduct the degradation of the pollutant at room temperature. This is a considerable economic advantage with respect to other technologies, although already known for their efficacy, which require the use of high temperatures, such as incineration. Another significant advantage that the UV technology potentially presents, is the absence of reaction subproducts, such as process water, sludges or solid beds to be treated and/or to be disposed.

This study was realized by designing and building up a system in which it was possible to verify the effectiveness of the UV and ozone technology on the abatement of volatile sulfur compounds. This was obtained by changing and measuring the main process parameters such as humidity, inlet pollutant concentration, residence time, temperature and residual ozone.

As reference sulfur compound for this study, hydrogen sulfide was chosen because it presents a high representativity for the case, due to the features previously described. [10].

Chapter 2

Volatile sulfur compounds

2.1 Sources

VSCs' sources can be both natural and anthropogenic [6]. The most common malodorous compounds are: hydrogen sulfide (H_2S), dimethyl sulfide (Me_2S), dimethyl disulfide (Me_2S_2), methyl mercaptan ($MeSh$), carbon disulfide (CS_2) and carbonyl sulfide (COS).

Table 2.1 shows the typical values associated to the main characteristics of each compound. These characteristics are:

- TLV: the Threshold Limit Value of a substance is the level to which it is believed a worker can be exposed a day after day for a working lifetime, without adverse health effects.
- Bp: boiling point of the substance at atmospheric pressure
- OT: the Odour Threshold corresponds to the minimum concentration of the substance in air, that can be detected by a human nose [11].
- STEL: the Short Term Exposure Limit is the acceptable average exposure over a short period of time, usually 15 minutes, as long as the time-weighted average is not exceeded.

For what concerns the natural sources, H_2S and Me_2S are the most produced compounds. They are particularly involved every time degradation of organic matter

Table 2.1 – Malodorous sulfur compounds summarized characteristics

Compound	Bp(°C)	OT(ppmv)	STEL(ppmv)	TLV(ppmv)
H ₂ S	−60.71	4.7x10 ^{−4}	15	10
MeSH	6.2	2.1x10 ^{−3}	0.5	—
Me ₂ S	37.3	1x10 ^{−3}	10	—
Me ₂ S ₂	198.7	9x10 ^{−3}	0.5	—
CS ₂	46.2	0.21	4	12

takes place under anaerobic and strongly negative redox potential conditions. Moreover the presence of VSCs is due to the degradation of sulphur compounds of biological origins, such as proteins (cysteine) [6].

The anthropogenic sources are more heterogeneous than the natural ones. Some industrial processes which present production of VCSs due to anaerobic conditions are: WWTPs (mainly H₂S), animal breeding stations, landfills, sludge decomposition facilities, anaerobic digesters and production of mushrooms cultivation substrate[6]. Moreover, it is generally possible to find sulfur compounds in any process that involves the heating of organic matter like rendering plants and food production industrial facilities (i.e roasting of coffee) [6].

Other sources of VSCs, related to the anaerobic decay or simply their direct usage for industrial applications are: manufacturing of viscose rayon, cosmetic industry, production of cellophane and fungicides, usage as solvents and addition as odour agent to natural gas[7]. The main technologies currently available in the field of the malodorous gases treatment and their functionings are described in the sections 2.2.1.1-2.2.2.2. The main advantages/disadvantages associated to them are briefly summarized in table 2.2, at the end of the next section.

2.2 Current treatment technologies for volatile sulfur compounds

2.2.1 Physicochemical methods

2.2.1.1 Scrubbing

Scrubbing systems are based on the transfer of pollutants from the gaseous to the aqueous phase; for this reason the parameter of interest is the pollutant volatility (defined by Henry's law). The treatment consists in a column in which the contact between gas phase and water phase is maximized by nebulizers. Since not all the compounds have a strong solubility in water, to improve the removal efficiency, it is necessary to enhance the solubility through the pre-oxidation of the pollutants in the gas stream (oxidative scrubbing) or by changing the pH of the process (alkaline scrubbing)[1].

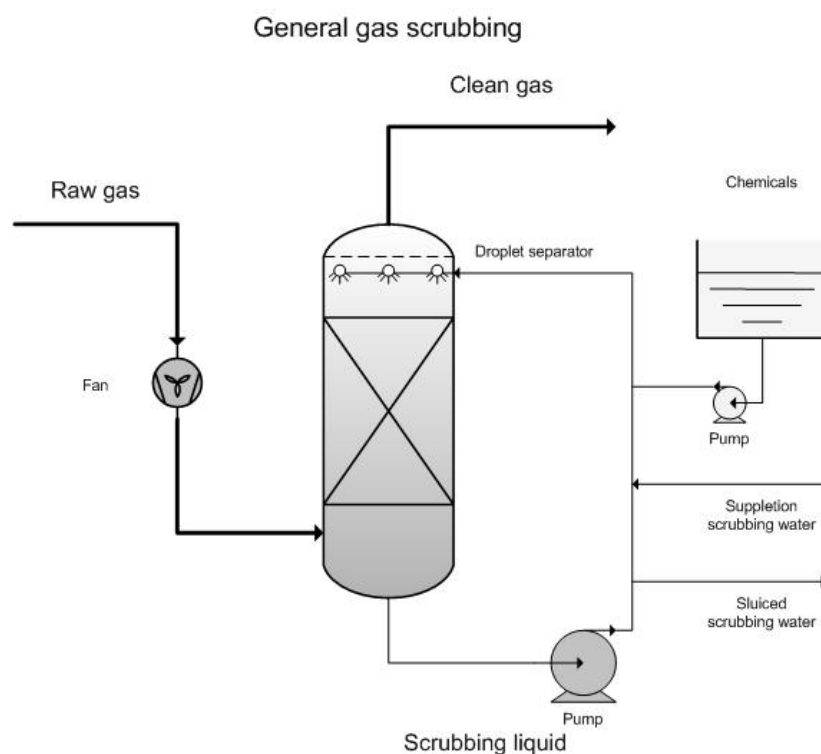


Figure 2.1 – Process scheme of gas scrubbing.[1]

2.2.1.2 Adsorption

Adsorption is a surface phenomenon, since it is based on the transfer of the pollutant from the gas phase to the solid phase. The solid phase, the adsorbent bed, is constituted by a granular porous material and its retention capacity is related to its specific surface and to the dimensions of the porosities that characterizes it (macro porosities, meso porosities and micro porosities). Different sizes of pores can adsorb different pollutant molecules[12]. The most used adsorbent is the activated carbon (AC) because its heterogeneous porosity and the relative cheapness makes its usage very flexible [13]. Other more specific and expensive adsorbents are silica gel zeolites and activated alumina. All adsorbents beds must cyclically undergo a regeneration process in order to partially restore the adsorption capacity. The adsorption capacity is the ratio between the maximum removable mass of the pollutant per mass of adsorbent bed. The working capacity of adsorbents in a regenerative installation in effect is lower than that of fresh adsorbents (50% for AC e 50-80% for zeolites)[1]. The desorption process can take place via pressure reduction, temperature increase or a combination of both. It normally takes place using steam, hot air or hot inert gas and, all the gases that are released during desorption, must be further treated. This aspect, combined to the electricity usage, strongly influence the operative costs of adsorption[1].

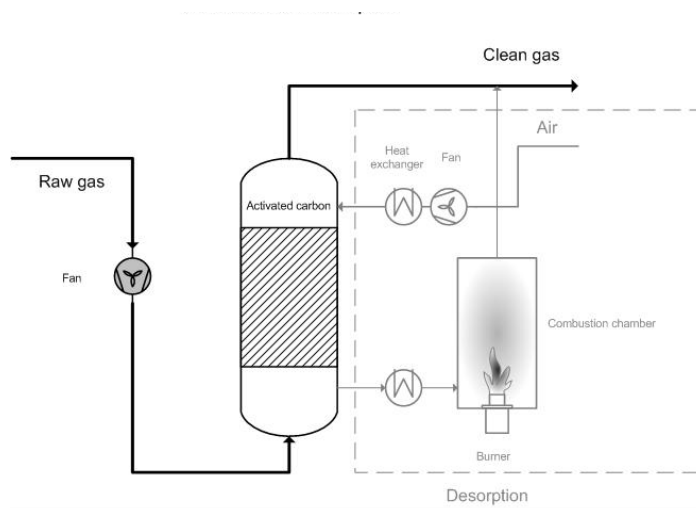


Figure 2.2 – Adsorption reactor configuration[1]

2.2.1.3 Incineration

The incineration is one of the most efficient and proven technology to treat waste gas in general because it lets not only the phase transition of the pollutants but their destruction or their conversion into less dangerous forms [6]. In order to do this, the system must be kept at high temperature; from 700°C to 1000°C for thermal incineration and from 300 to 400 C for catalytic incineration. This technology presents a high variability of the costs in presence of low concentrations of pollutants and, in general, the little flexibility in presence of possible fluctuation of the flow rates and concentrations in entrance [1].

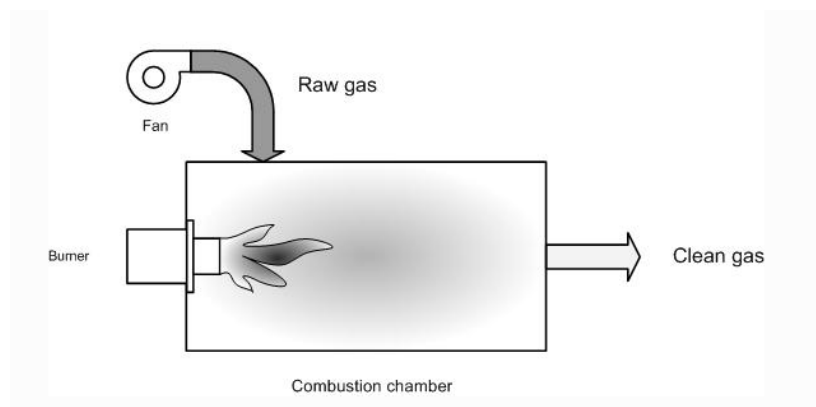


Figure 2.3 – Incineration system configuration[1]

2.2.2 Biotechnological methods

They include biofilters, bioscrubbers and biotrickling filters[7]. These systems are generally based on two main steps: the first one is the adsorption of the volatile contaminants in the aqueous phase or in a biofilm and the second step is the consequent biodegradation of the sorbed pollutant by selected microorganisms. When specific compounds must be removed, the inoculation of specialized microorganisms is needed.

These systems generally require a secondary source of nutrients, besides a carbon source, and additional water (where it is needed, for example in biofilters). For this purpose, a mix of nutrients is added: nitrogen, phosphorus and trace elements in the right proportions [1]. Moreover, in order to keep an adequate oxygen level to let the

aerobic degradation continue, an aeration device must be present.

2.2.2.1 Biofilters

In this system the gas is passed upwards through a filter bed, which has been constructed with biological material (compost, tree bark or peat). In this structure the first retention step occurs. The degradation step is conducted by microorganism which are localized in a thin film of water on the filtering material[8].

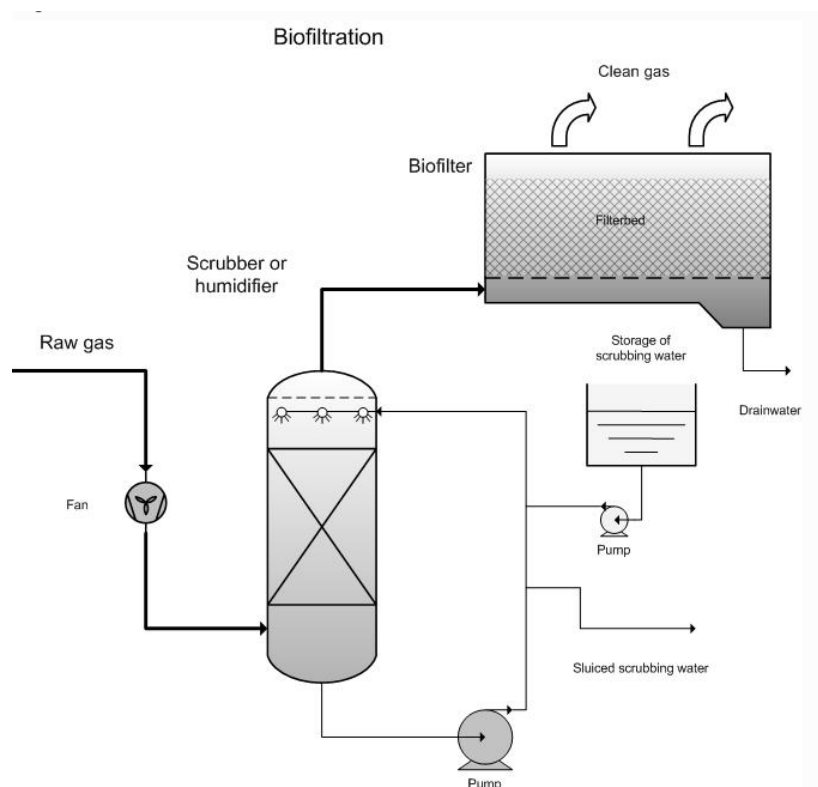


Figure 2.4 – Biofiltration reactor configuration[1]

2.2.2.2 Bioscrubbers

The bioscrubber is basically constituted by a scrubber followed by a biological reactor [8]. In the gas scrubber, the pollutants are absorbed from the gas stream by the washing water. In the biological reactor, pollutants in wash water are biologically degraded and the purified scrubbing liquid is sent again to the scrubber in order to be recirculated. Usually, stable flue gas streams are preferred, both in terms of composition and load.[6]

Usually, stable gas streams are preferred, both in terms of composition and load.^[6]

Another important aspect that must be considered is the production of sludge and discharge water that need to be further treated or disposed of.

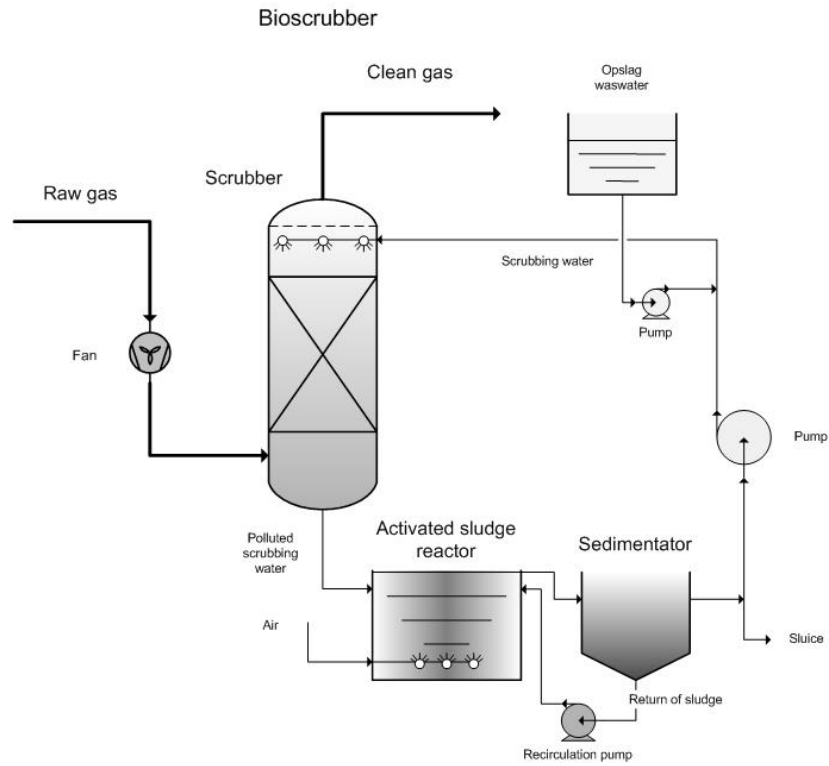


Figure 2.5 – Bioscrubber reactor configuration^[1]

Table 2.2 – Advantages and disadvantages of the current technologies available for odour treatment caused by VOCs [6][1] [7] [8].

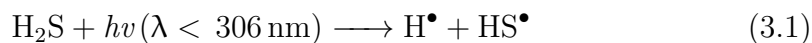
Technology	Advantages	Disadvantages
Scrubbing	Oxidation of several compounds beside sulfur ones, fairly efficient.	Process water to be treated, sodium hypochlorite is a dangerous and corrosive substance (oxidative scrubbing).
Adsorption	High adsorption capacity towards VSCs, simple and robust technology, easy to maintain and to place.	Non continuous process (regeneration), pre/post treatment may be required, risk of spontaneous combustion in the bed.
Incineration	Efficient and proven waste gas technology, not phase transition but destruction of pollutants.	High variable costs for fuels with low concentrations, fuel consuming, formation of corrosive acid gases.
Biofilter	Low investment and operation costs, simple construction, little waste water (percolate).	Large surface area needed, periodical replacement, few configuration parameters to improve efficiency, risk of clogging, need of constant aeration of the bed.
Bioscrubber	Degradation of components, no transition of phase.	Pollutants must be water soluble, stable flue gas streams preferred, production of sludge.

Chapter 3

Hydrogen sulfide removal mechanism in the photoreactor

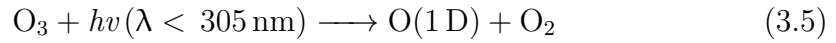
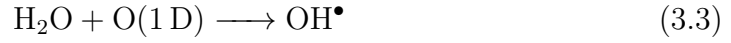
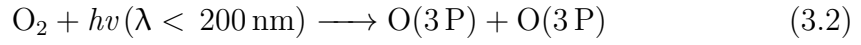
The removal mechanism of H_2S in air, in condition compatible with those of the study conducted, is ruled by several phenomena. As seen in [14], in presence of oxygen, humidity and UV light, these phenomena are:

- **Direct photolysis:** the photodissociation of H_2S , that has been previously studied in [15], can occur when energy higher than $385.92 \text{ kJ mol}^{-1}$, corresponding to a wavelength of 309 nm , is absorbed by hydrogen sulfide with its consequent dissociation. The mechanism follows the reaction:



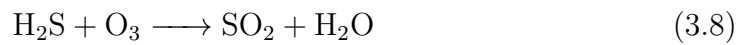
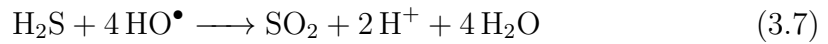
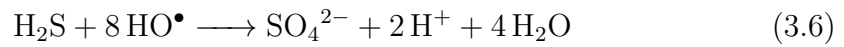
- **indirect photolysis by O_3 and OH^\bullet :** since the photo energy of UV light at 185 nm is capable of splitting the $\text{O}=\text{O}$ bond, in presence of Oxygen, moisture and UV light, the removal of Hydrogen Sulfide also depends on the O_2 -mediated generation of OH^\bullet and O_3 .

The generation of O_3 and OH^\bullet is shown in the following equations:

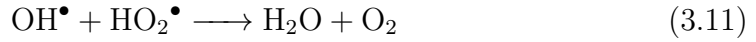
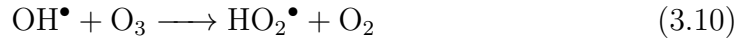


The wording 1D, 3P, etc. indicates a particular chemical form defined as “singlet”. The different notation refers to the energy corresponding to free orbital of a given atom. It is important to underline that the form 1D has a higher energy than the form 3P.

- **The dissociation of H_2S :**



- Scavenging/competitive reactions [16, 17]:



- **The absorption of UV light by water:** as seen in [2] the relative humidity (RH) influence the ozone production because the 185 *nm* radiation is absorbed by H₂O and O₂. Picture 3.1 shows the magnitude of this influence. This picture, in particular, shows how under several different conditions of flow rates, O₂ concentrations and humidity contents, there is a general trend that relates RH and residual ozone after the permanence in the photoreactor. As it is possible to see in all the graphs presented, the highest humidity corresponds to the lowest residual ozone.

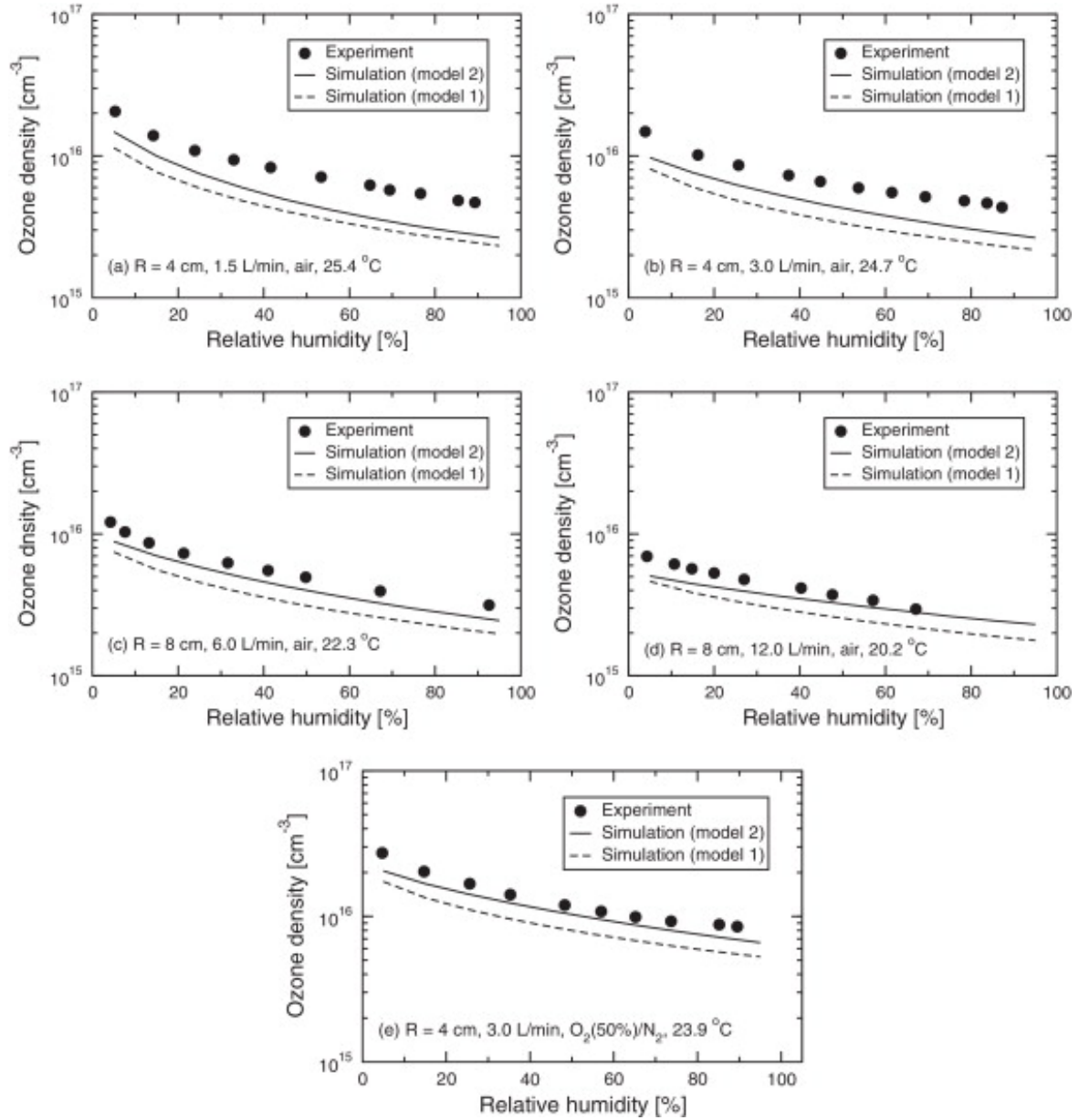


Figure 3.1 – Comparison of the ozone densities obtained from simulation and experiments under different humidity, O_2 concentration, and flow conditions[2].

Chapter 4

Experimental planning

4.1 Main parameters

The aim of the project is to test the effectiveness of the photo oxidation as a new technology for the degradation of hydrogen sulfide. Since in literature it is possible to find very few papers related to this specific field, all the results that have been collected constitute an important first data background for the study of the behavior of this compound under different conditions. For this reason, the parameters that were chosen to be controlled, in order to create a heterogeneous range of conditions, as similar as possible to real cases (e.g. WWTPs), are: humidity, residence time and inlet concentration of pollutant.

It is important to underline that, since the experiments were conducted in a laboratory, it was necessary to operate a down scale (e.g. maximum flow rate of 30 *l/min* and maximum inlet concentration of 100 ppm), in order to obtain a more accurate control of all the conditions, still keeping the correct proportions among them. On the other hand, the parameters that were monitored are: temperature of both the lamp and the reactor and residual ozone.

To summarize, the tests were conducted with the following conditions:

- **Flow rate:** for the reactor used for the experiments, the different flow rates chosen for this study, correspond to the residence times shown in Table 4.1.

Table 4.1 – Relation between flow rates and residence time in the reactor.

Flow rate [l/min]	Residence time (τ) [s]
5	9.87
15	3.29
20	2.47
30	1.70

In order to calculate the residence time, first it was necessary to calculate the inner volume of the reactor. Considering the dimensions shown in Picture 4.1, it was calculated as:

$$V_{reactor} = \left(\frac{\pi D_{in,steel}^2}{4} - \frac{\pi D_{ext,quartz}^2}{4} \right) \cdot L_{reactor} \quad (4.1)$$

- $V_{reactor}$: inner volume of the steel reactor (cm^3)
- $D_{in,steel}$: inner diameter of the steel reactor (cm)
- $D_{ext,quartz}$: external diameter of the quartz sleeve (cm)
- $L_{reactor}$: length of the steel reactor (cm)

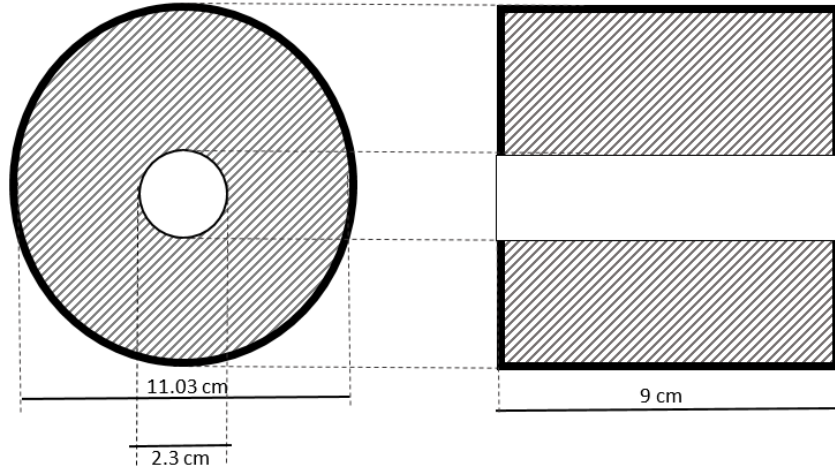


Figure 4.1 – Sizes of the photoreactor

The inner volume of the reactor resulted to be 822.6 cm^3 . Thus, the residence time inside the reactor was calculated as:

$$\tau = \frac{V_{\text{reactor}}}{Q} \cdot \frac{60}{10^3} \quad (4.2)$$

- τ : residence time (s)
 - V_{reactor} : inner volume of the steel reactor (cm^3)
 - Q : flow rate (l/min)
- **Relative humidity:** the parameter measured during all the tests is relative humidity (RH). Compared to absolute humidity, which is more difficult to measure, since it changes with the pressure and the temperature, the RH is more suitable to be measured, since it is defined as the ratio of the partial pressure of water vapour in the mixture to the saturated vapor pressure of water at a given temperature. Thus the relative humidity of air is a function of both water content and temperature [18].

In industrial scenarios the RH varies in a wide range but, usually, the average values don't exceed the 70% [19].

For this project, different humidity content were applied, in the range of 20%–85%.

- **Temperarure:** all the tests were conducted at room temperature, then without the aid of heating systems.

It is important to underline that for some tests, some parameters have been voluntarily pushed to uncommon levels, not compatible with real/industrial cases, to enhance the performance differences between different experiments and in order to understand better the nature of the phenomena involved in the process.

4.2 Preliminary tests: methodology

In order to test the operativity of the system, to find any problems in the system and to troubleshoot the system, some preliminary tests with acetaldehyde were carried out. Acetaldehyde was chosen since it was already available in the laboratory and because, in other previous tests [20], it showed to have a very high stability towards the photooxidation. This last feature, combined with lower dangerousness if compared to H_2S , made it the best compromise for these first tests, because any small degradation seen for acetaldehyde it was theoretically expected to correspond to higher H_2S conversion, when running tests in the same conditions.

The first step consisted in finding an appropriate flow rate to use for the experiments. For this reason, the first series of tests were conducted without humidification system and the flow rate that first presented a degradation of a certain relevance (not attributable just to systematic errors) was chosen. In this case 5 l/min , corresponding to a residence time of 9.87 s , was chosen.

Once fixed the flow rate, three series of test were conducted for different RH percentages (50, 60 and 85%) , by measuring the degradation of acetaldehyde obtained with different concentration fed to the reactor (30, 50, 70, 90, 100, 150, 200 ppm).

4.3 Tests with hydrogen sulfide: methodology

For the tests on hydrogen sulfide a similar procedure to acetaldehyde's one was used. Three flow rates were chosen: 15 l/min , 20 l/min and 30 l/min , in order to be as similar as possible to the real cases but still considering the laboratory scale limitations and in order to evaluate the influence of the residence time in the process. This purpose was pursued by using a realistic UV power/ flow rate ratio (using the maximum flow rate available in lab scale, 30 l/min and a small UV lamp 6 W), based on the suggestions of the partner company collaborating to the project. This ratio was for example much higher than that found literature [14].

Once fixed the flow rate (15 l/min , 20 l/min or 30 l/min), three series of test were conducted for different humidity percentages (21, 40 and 60%), by measuring the degradation of hydrogen sulfide obtained with different concentration fed to the reactor (20, 35, 50, and 70 ppm), in the range of the odor perception. The 21% of RH was chosen as minimum value because it was the lowest allowed in the laboratory.

All the tests were conducted at room temperature (the temperature inside the reactor kept itself around $25\text{-}27\text{ }^{\circ}\text{C}$) and, as additional parameter, the residual ozone produced by the lamp was measured.

Chapter 5

Experimental setup

5.1 System configuration

The system configuration was designed taking as reference some examples of similar applications found in literature [21, 22, 23]. It was constituted by:

- **Feeding section:**
 - H₂S bottle
 - Compressed air line inside the laboratory
- **Photoreactor:**
 - Stainless steel external structure
 - Quartz sleeve
 - Low pressure ozone generating UV lamp
- **Humidification system**
 - Washing bottles
 - Thermostated water bath
 - Hygrometer
- **Condensation system**

- Bulb condenser
- Ampoule for condensed water collection
- **Analysis section**
 - Gas analyzer
 - Ozone detector

The gas flow, composed by a controlled mix of hydrogen sulfide, air and water vapour, passed throughout the photoreactor, containing the UV ozone generating lamp. After this, an ozone analyzer monitored the residual ozone after the photoreaction. Then, after a condensing system constituted by a glass water cooling condenser, the residual concentration of the pollutant analyzed was detected by the appropriate gas analyzer, see section 5.2.5. The structure of the system is schematized in Figure 5.1, while Figure 5.2 shows a picture of the system.

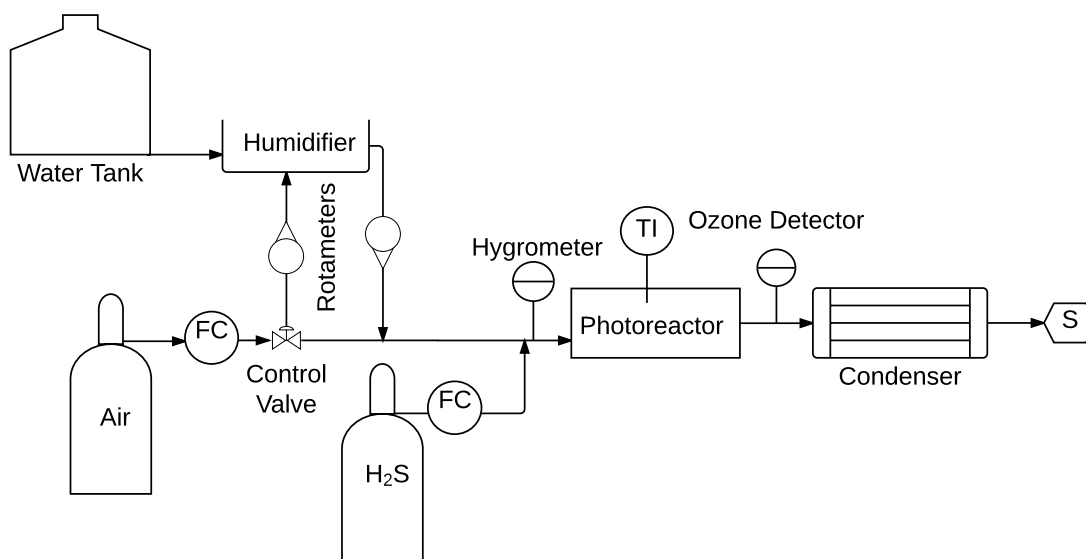


Figure 5.1 – P&ID system scheme of oxidation using UV light producing ozone

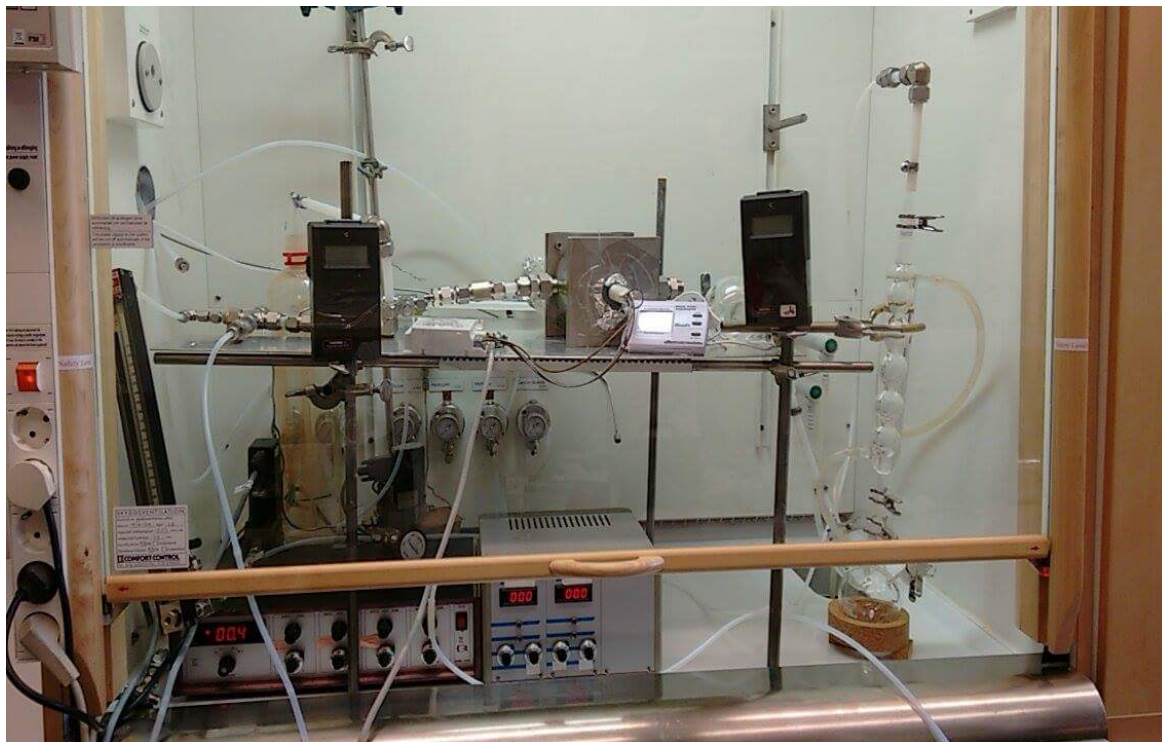


Figure 5.2 – Photo of the complete system

5.2 Instruments and devices

5.2.1 Gas supply system

The supply system was entirely constituted by teflon tubes and stainless steel fittings in order to prevent corrosion phenomena and adsorption on the inner walls of the pipes, due to the presence of hydrogen sulfide.

The inlet concentration of the compound to remove was regulated by changing the values of the two main flow rates: compressed air and chemical compound (acetaldehyde or hydrogen sulfide). The flow rates were controlled by two analogic mass flow controllers (for H_2S or acetaldehyde, and air) and by two rotameters to adjust the ratio of humid and dry air. Each mass flow control device was calibrated using a bubble mass flow controller.

5.2.2 Humidification system

The humidification system was realized with two impinger bottles, filled with deionized water, in which the compressed air flows upstream through a microporous filter made of sintered glass, in order to create micro bubbles. The two bottles were immersed in a thermostated water bath, in order to keep the temperature around 80 °C and enhance the humidification effectiveness.

A system of valves allowed controlling the humidity in the overall gas stream going into the reactor, regulating the ratio between dry and humid air. Figure 5.3 shows a picture of the humidification system.



Figure 5.3 – Humidification system

5.2.3 Devices for main parameters control and monitoring

The temperature was constantly monitored in the interspace between the lamp and the quartz sleeve, in order to prevent the overheating of the lamp, and inside the steel reactor, in order to control the temperature of the gas stream during the oxidative process. This operation was done using two Pentronic thermocouples of different sizes. In particular, the temperature of the lamp was kept in the right range (50-55°C)

regulating the flow rate of a cooling air flux in the quartz sleeve.

The humidity in the gas stream was monitored just after the photoreactor, placing an hygrometer probe, model Wood's SS7002, inside a glass vial in which the gas stream was conveyed. The hygrometer provided the temperature in the vial too, allowing the calculation of the vapor pressure of the water to quantify the contribute of the water to the overall flow rate. It is important to underline that during all the experimental campaign, no condensation of water was observed, probably due to the low ambient temperature kept in all the process. Figure 5.4 shows a picture of the hygrometer probe inside the glass ampoule.

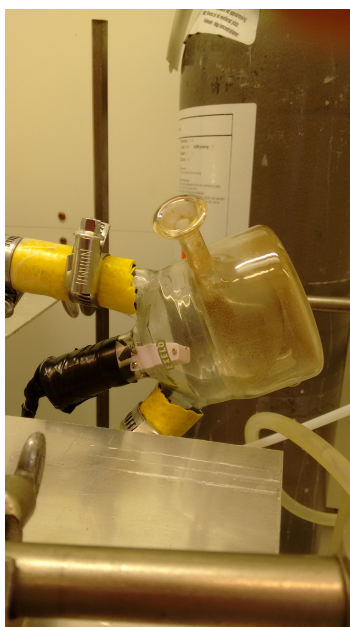


Figure 5.4 – Photo of the glass ampoule containing the hygrometer probe

5.2.4 Photoreactor

5.2.4.1 Stainless steel reactor

The main structure of the photoreactor, Figures 5.5 and 5.6, is cylindrically shaped and made of stainless steel (EN 14404), a particular alloy with a high resistance to corrosion, and designed considering the length of the lamp, 9 cm, the maximum flow rate reachable on a laboratory scale, 30 l/min, and keeping a minimum residence time

of 1.5 *sec*. The resulting inner volume of the reactor is 822.6 cm^3 . The steel structure presents two axially aligned holes to support the high purity quartz sleeve that has the aim to support and to protect the UV lamp. The inlet and the outlet pipes of the gas stream are placed radially in opposite position and, respectively, at the beginning and at the end of the cylindrical body, to ensure a certain turbulence to the system.

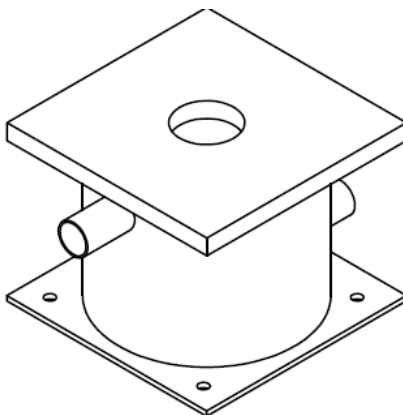


Figure 5.5 – Drawing of the stainless steel body of the photoreactor obtained with the software Autodesk Inventor

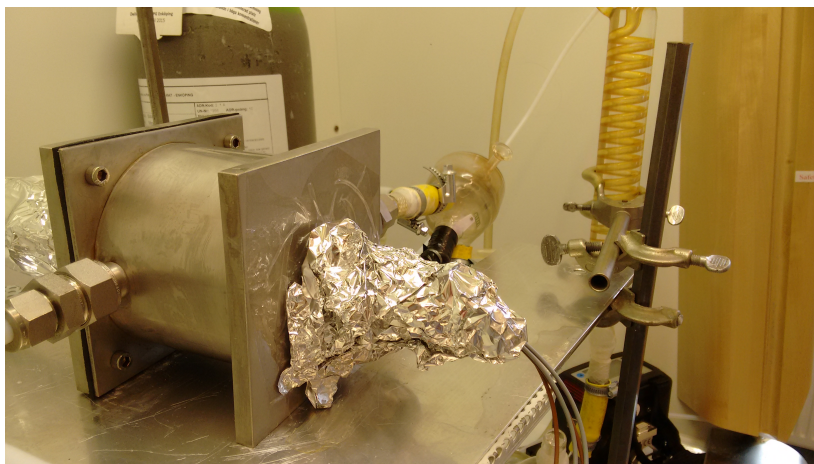


Figure 5.6 – Stainless steel photoreactor

5.2.4.2 UV lamp

The UV lamp that was placed inside the quartz sleeve was an Heraeus GPH150T5VH/4, a mercury low pressure ozone generating lamp, characterized by a power supply of 6 W and a light emission at 185 and 254 nm. See figure 5.7. This lamp was chosen for this project because ozone is known to be a very reactive compound and the study of its behaviour under the conditions kept during the experiments conducted, is one of the objectives of this project. Figure 5.8 shows the wavelength distribution of the lamp.



Figure 5.7 – Heraeus GPH150T5VH/4 lamp

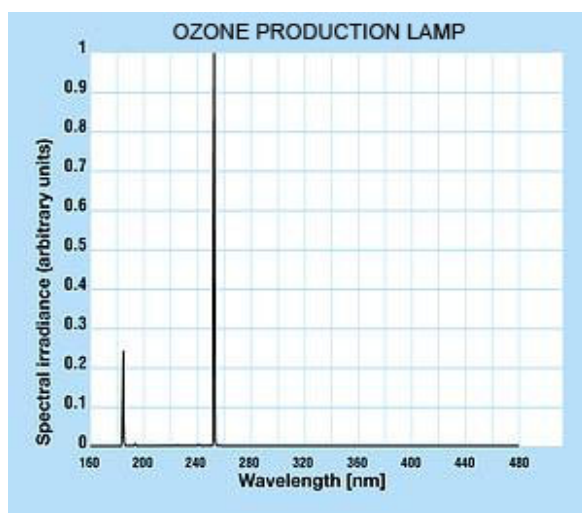


Figure 5.8 – Wavelength distribution of the mercury low pressure ozone generating lamp

5.2.5 Gas analyzers

5.2.5.1 X-am 7000

A Dräger X-am 7000 sensor was used to evaluate the concentration of acetaldehyde after the photooxidation during the preliminary tests. This device is usually used for the detection of VOC in air. In this case it was equipped with a PID (Photo Ionization

Detector), a sensor that can give a quick response in the range of ppm. The air is drawn into the measuring chamber through the gas inlet. In the chamber, a UV lamp produces photons, which ionize certain molecules within the flow of gas. Then the molecules are subjected to the electrical field between two electrodes in the measuring chamber. The strength of the resulting current is directly proportional to the concentration of ionized molecules inside the chamber. This makes it possible to determine the concentration of the substance in the air [3]. See Figure 5.9.

The PID sensor was calibrated with Isobutylene, a non-hazardous gas and available in practical disposable test gas cylinders. The sensitivity of acetaldehyde can be set through response factors. If a substance is detected with greater sensitivity than Isobutylene, then its response factor is less than one. Substances that are detected with less sensitivity than Isobutylene have a response factor greater than one. Thus, it was possible to calibrate the sensor as explained in section 6.1.

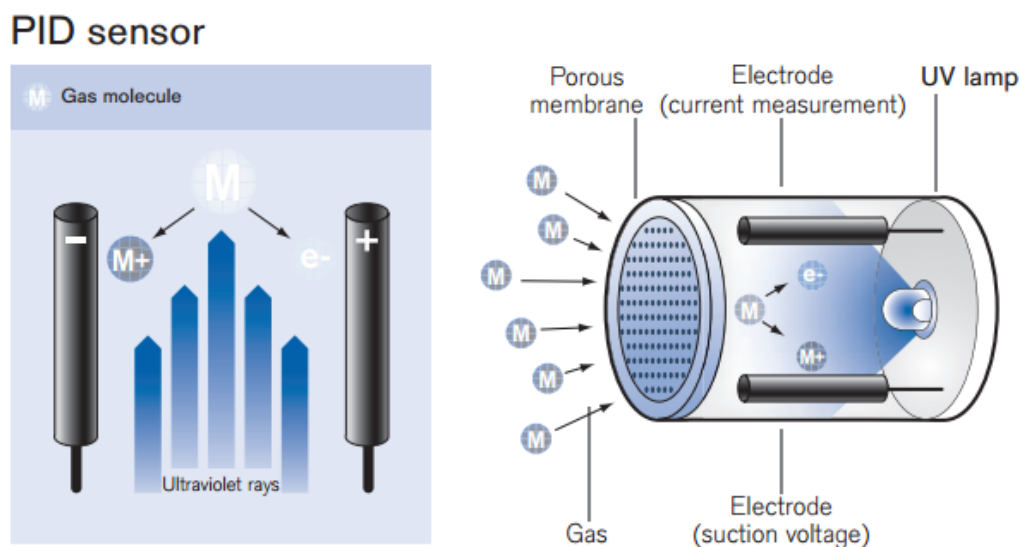


Figure 5.9 – Operating diagram of the PID sensor [3]

5.2.5.2 Gas Chromatograph

An Agilent Gas Chromatograph (GC) 6890 in combination with the Agilent Sulfur Chemiluminescence Detector (SCD) was used for the evaluation of the hydrogen sulfide

concentration. The system composed by these two instruments it is shown in Figure 5.10.

The GC 6890 is gas chromatograph and it is constituted by the following components [4]:

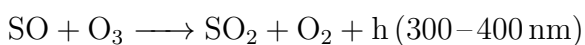
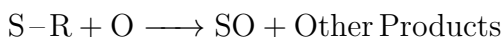
- Gas supply for carrier gas (cylinder, generator)
- Injector (injector port)
- Oven with the column
- Detector
- Data Acquisition System (PC or Recorder)

Its functioning is based on the following principle: the separation accomplished by partitioning of different volatilized substances between a mobile carrier gas (helium, in this case) and a stationary phase. If one phase is stationary, the coating, and the other is moving, the carrier gas, the component will travel at a speed less than that of the moving phase. The speed depends on the strength of the attraction. If different components have different attractions with the column, they will separate in different reaction times [4].

The separation is done on a capillary column, an Agilent GS- Gaspro, which is housed in the oven of the gas chromatograph.

The Agilent SCD was used as detector. It utilizes the partial oxidation of sulfur compounds to form sulfur monoxide (SO) and chemiluminescence reaction of SO with ozone (O₃). The oxidation process achieves high temperatures (>800 °C). The SCD can make ultra-sensitive measurements of any sulfur-containing compound that can be analyzed by gas chromatography.

The reaction mechanism is:



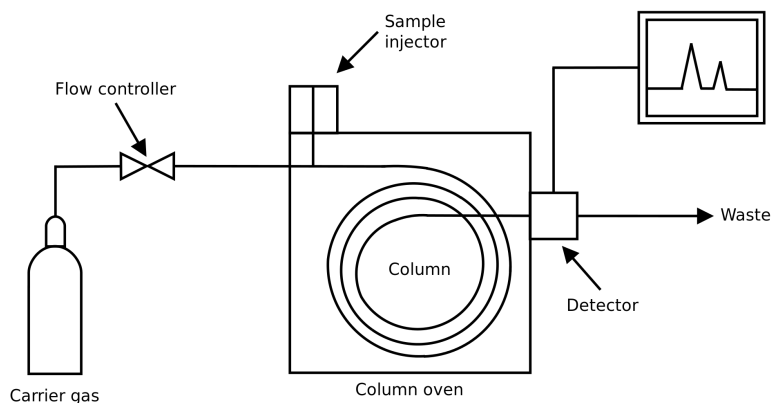


Figure 5.10 – Simplified scheme of the system composed by a GC followed by a SCD [4]

The light passes through an optical filter and is detected by a photomultiplier tube. The light emitted is directly proportional to the amount of sulfur in the sample.

The results obtained are shown in a chromatogram in which each peak, that appears at different typical reaction time of the analysis, corresponds to a different compound. The integration of a peak allows calculating the area under it, that it is directly proportional to the concentration of the compound detected. An example of a chromatogram is shown in Figure 5.11.

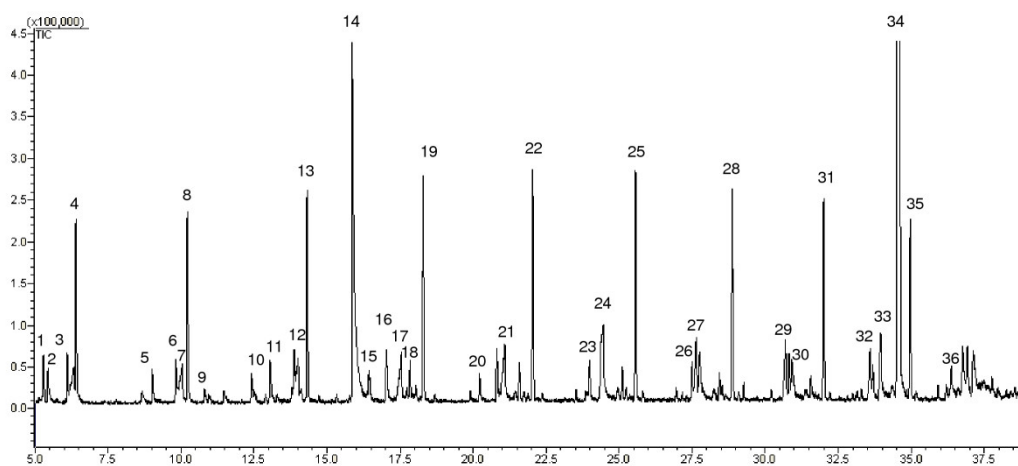


Figure 5.11 – Figure showing the typical appearance of a chromatogram sequence

5.2.5.3 Ozone Detector

A 2B Technologies ozone monitor model 106-L was used in order to quantify the residual ozone after the photochemical process.

This device works basing on the principle of ozone absorption by ultraviolet light at 254 nm. Ozone is measured based on the attenuation of light passing through a 14-cm absorption cell fitted with quartz windows. A low-pressure mercury lamp emitting at 254 nm is located on one side of the absorption cell, and a photodiode is located on the opposite side of the absorption cell [24]. The detection in air extends over a wide dynamic range (from some ppb up to 100 ppm).

5.2.6 Safety equipment

Since both acetaldehyde and hydrogen sulfide have a toxic and/or cancerogenic risk or flammable and explosive properties, it was necessary to provide a safety equipment, additional to the air recirculating system that was already present in the laboratory.

The safety equipment was composed by a breathing mask, equipped with adequate filters (ABE1K), eye goggles and alarm gas sensor to monitor the concentration of the dangerous pollutants in the air.

Chapter 6

Results

6.1 Preliminary tests

To analyze the outlet concentration, the Xam-7000 was used. As mentioned before, this instrument is equipped with a PID sensor that it is calibrated using isobutylene so the value shown on the instrument needs to be corrected using a conversion factor, in order to obtain the concentration of acetaldehyde.

This conversion factor was obtained through some tests with the UV lamp switched off, with a known and controlled concentration of acetaldehyde fed into the system. For each concentration the number shown on the PID was read. In this way a series values of the PID were obtained for each corresponding concentration. Subsequently the same operation was done even for different humidities in the system. It is possible to see an example in Figure 6.1. The points obtained were linearly interpolated to allow the determination of the concentration of acetaldehyde for any PID value.

This operation implies a loss in the accuracy since a small variation of one unit on the sensor can corresponds to a variation of about plus/minus 5 ppm in the real acetaldehyde concentration. In this way small degradations are not detected.

It is important to underline that at this phase of the study the main purpose was to see the qualitative behaviour of the degradation of the compound just to learn how to adjust the main parameters and to be able to find out technical errors or malfunctioning in the system configuration.

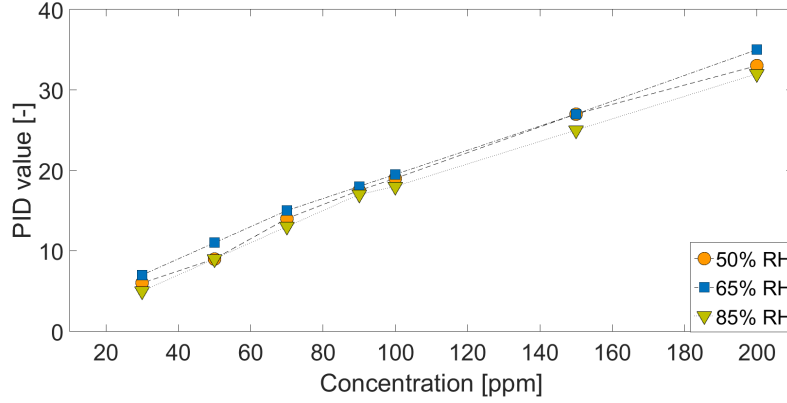


Figure 6.1 – Diagram showing the obtained calibration factor

Once fixed the flow rate and obtained the calibration factors for each concentration and for each humidity, the tests to analyze the degradation obtained for different inlet concentration and moisture in the air stream were conducted.

Each series of tests was conducted by keeping fixed the residence time and the humidity and changing the inlet concentration. As it is possible to see in Figure 6.2 the degradation reaches significant levels just for low concentration of acetaldehyde, while it decreases with the increasing of the concentration. Moreover, increasingly high values of humidity in the air stream seem to influence positively the degradation for low concentration of acetaldehyde while the influence runs off almost around zero with the increasing of the concentration. These results confirm the relative stability of acetaldehyde as already seen in previous tests [20].

$$X_i = \frac{C_{i,in} - C_{i,out}}{C_{i,in}} \cdot 100 \quad (6.1)$$

- X_i : removal efficiency of the i -compound [%]
- $C_{i,in}$: inlet concentration of the i -compound [ppm]
- $C_{i,out}$: outlet concentration of the i -compound [ppm]

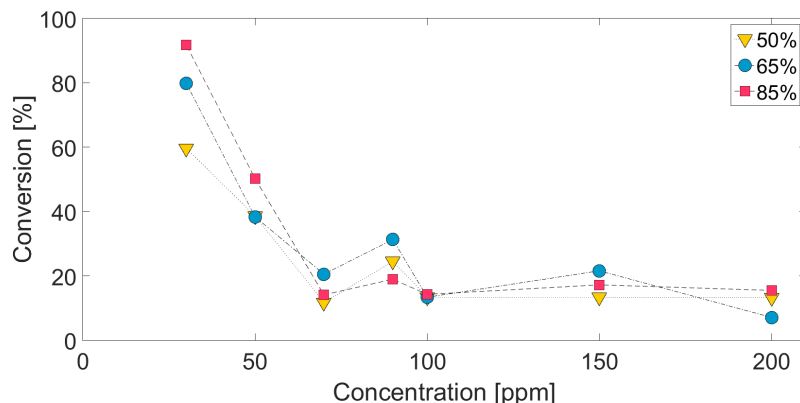


Figure 6.2 – Results of the tests conducted with different moisture grades

6.2 Hydrogen sulfide tests

Since the evaluation of the outlet concentration of hydrogen sulfide was done using a different gas analyzer from the one used for acetaldehyde, another calibration was necessary. As already seen in section 5.2.5 the concentration of the pollutants detected by the GC SDC is proportional to the area under the corresponding peak in the chromatogram generated during the test. For this reason, a series of known concentrations, was flown in the system and the corresponding areas were annotated in order to find the relation between the two parameters. Figure 6.3 shows the results of the calibration. As it is possible to see, the relation between peak area and concentration is practically linear.

During all the experimental campaign with H_2S , all the sample were taken after the complete stabilization of the system. Than as reference data, the average area obtained by three consecutive peaks in the chromatograms, in stable conditions, was taken into account.

All the data obtained are shown in Sections 6.2.1–6.2.3, while the discussion and the illustration of the hypotheses are described in Section 6.2.4.1.

The results obtained from all the series of test conducted are summarized in the following diagrams.

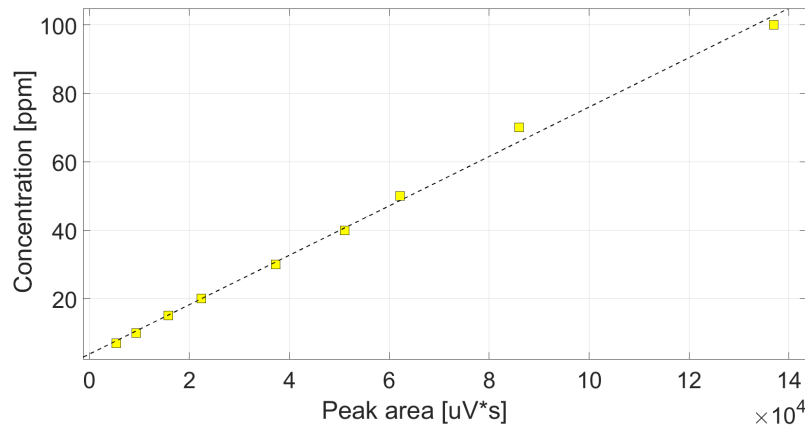


Figure 6.3 – Diagram showing the relation between the chromatogram area and the concentration

6.2.1 Comparison between different residence times

These three diagrams were obtained in order to emphasize the differences in degradation due to an higher or shorter residence time and search the relation between them. The residence times for the case studied are summarized in the table 6.1.

In particular, this first series of diagrams, shows the different conversions of H_2S , for each inlet concentration, obtained for different humidity conditions, given a fixed residence time.

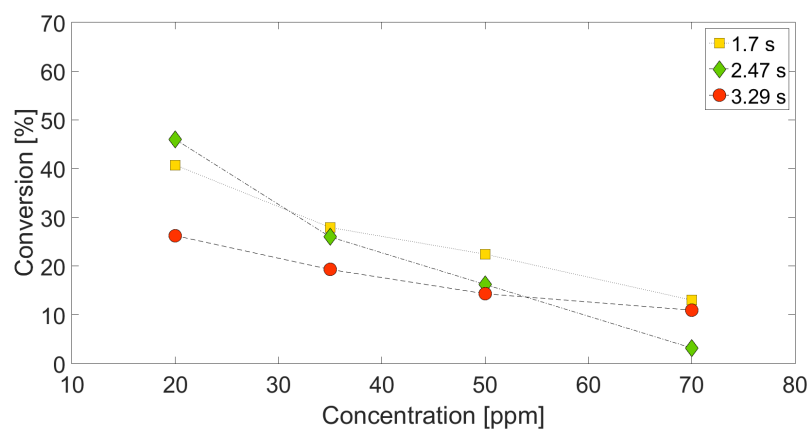
The result expected is usually a better conversion corresponding to a higher residence time but, as it is possible to see in diagram ??, obtained for a humidity content of 21% (the lowest allowed in the laboratory), this hypothesis was not confirmed. In fact, the degradation of H_2S for a residence time of 3.29 s, presents a trend that in the diagram is under those obtained for 2.47 s and 1.7 s, in terms of degradation.

On the other hand, the trend seems to take a more expected behaviour for higher humidity contents. Figure 6.5 shows how, for 40% of RH, the degradation is significantly better for 3.29 s compared to 2.47 s and 1.7 s, even if these last two trends are almost overlapping.

For 60% of RH the differences in the degradation trends, obtained for different residence times and flow rates, is even less visible. See Figure 6.6.

Table 6.1 – Relation between flow rates and residence time in the reactor.

Flow rate	Residence time (τ)
$[l/min]$	$[s]$
15	3.29
20	2.47
30	1.7

**Figure 6.4** – Comparison between the degradation obtained with different residence times for a condition of 21% of RH (the lowest allowed in the laboratory)

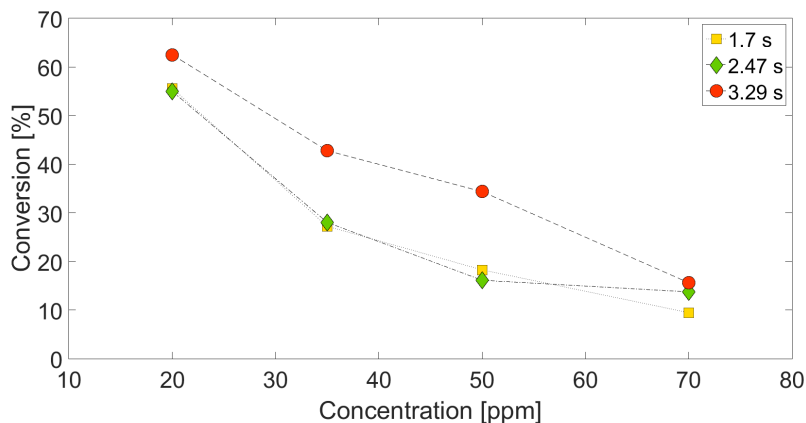


Figure 6.5 – Comparison between the degradation obtained with different flow rates for a condition of 40% of RH

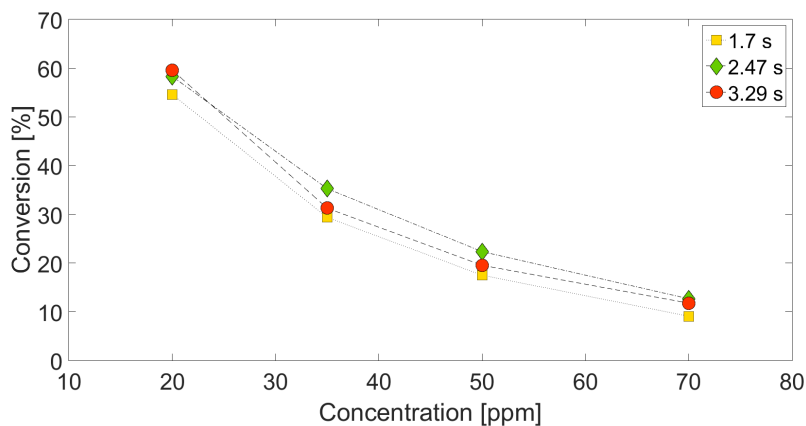


Figure 6.6 – Comparison between the degradation obtained with different residence times for a condition of 60% of RH

6.2.2 Comparison between different humidity contents

These three diagrams were obtained in order to emphasize the differences in degradation due to a different RH percentages, with a constant residence time. The expected result was a higher conversion corresponding to higher RH, since water enhances the production of OH radicals (reaction 3.3 and 3.5).

Looking at Figure 6.7 the behaviour is not the one expected, since the highest RH does not correspond to the highest conversion. Infact it is possible to see that the

conversion is generally better at 40% of RH than 60% of RH. The difference between the different conversion rates for different RH, is reduced as the inlet concentration increases. Moreover, as it is possible to see in Figure 6.8 and 6.9, as the residence time decreases, as RH is less influent in term of conversion.

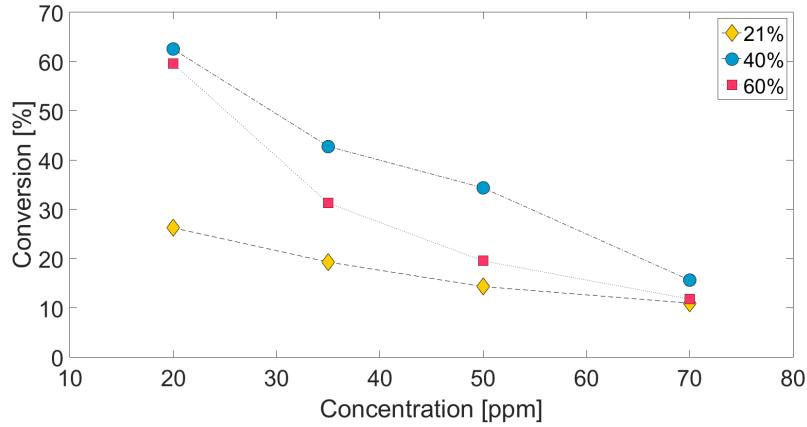


Figure 6.7 – Comparison between the degradation obtained with different RH with a given constant residence time of 3.29 s

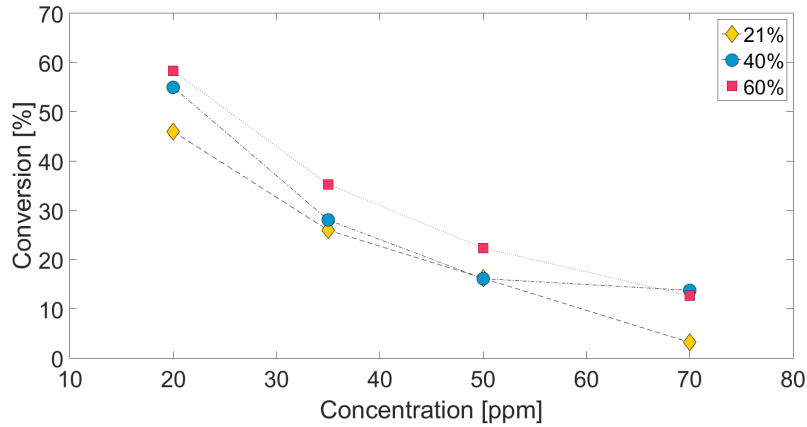


Figure 6.8 – Comparison between the degradation obtained with different RH with a given constant residence time of 2.47 s

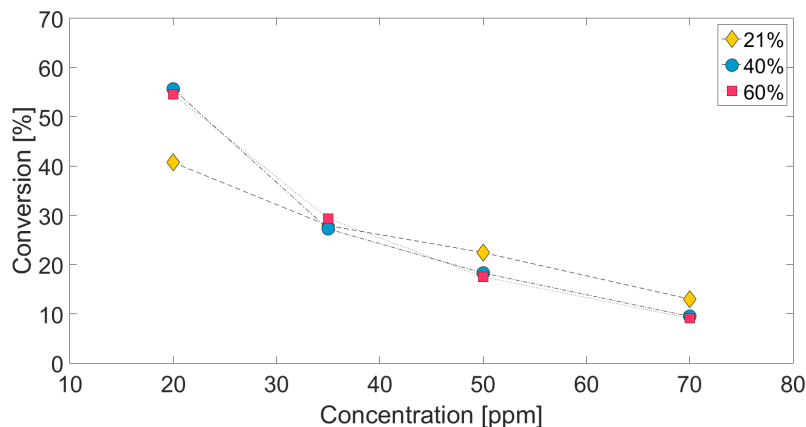


Figure 6.9 – Comparison between the degradation obtained with different RH with a given constant residence time of 1.7 s

6.2.3 Comparison between different inlet concentrations

In Figure 6.10, is shown the difference in degradation observed for different inlet concentrations. As it is possible to see, generally the conversion decreases as the inlet concentration increases. This distance is slightly accentuated for the tests conducted with high humidity content. However, as the inlet concentration increases, the effect of the different control parameters (humidity and residence time) is gradually damped, converging towards ever lower conversion rates. This effect is visible by comparing the data obtained for 20 ppm of H_2S fed into the reactor with those obtained for higher concentrations. Data referring to 20 ppm are more spread in the chart area, if compared with the others. This confirms that, for low concentrations of H_2S fed into the system, it is possible to see a bigger influence of the process parameters.

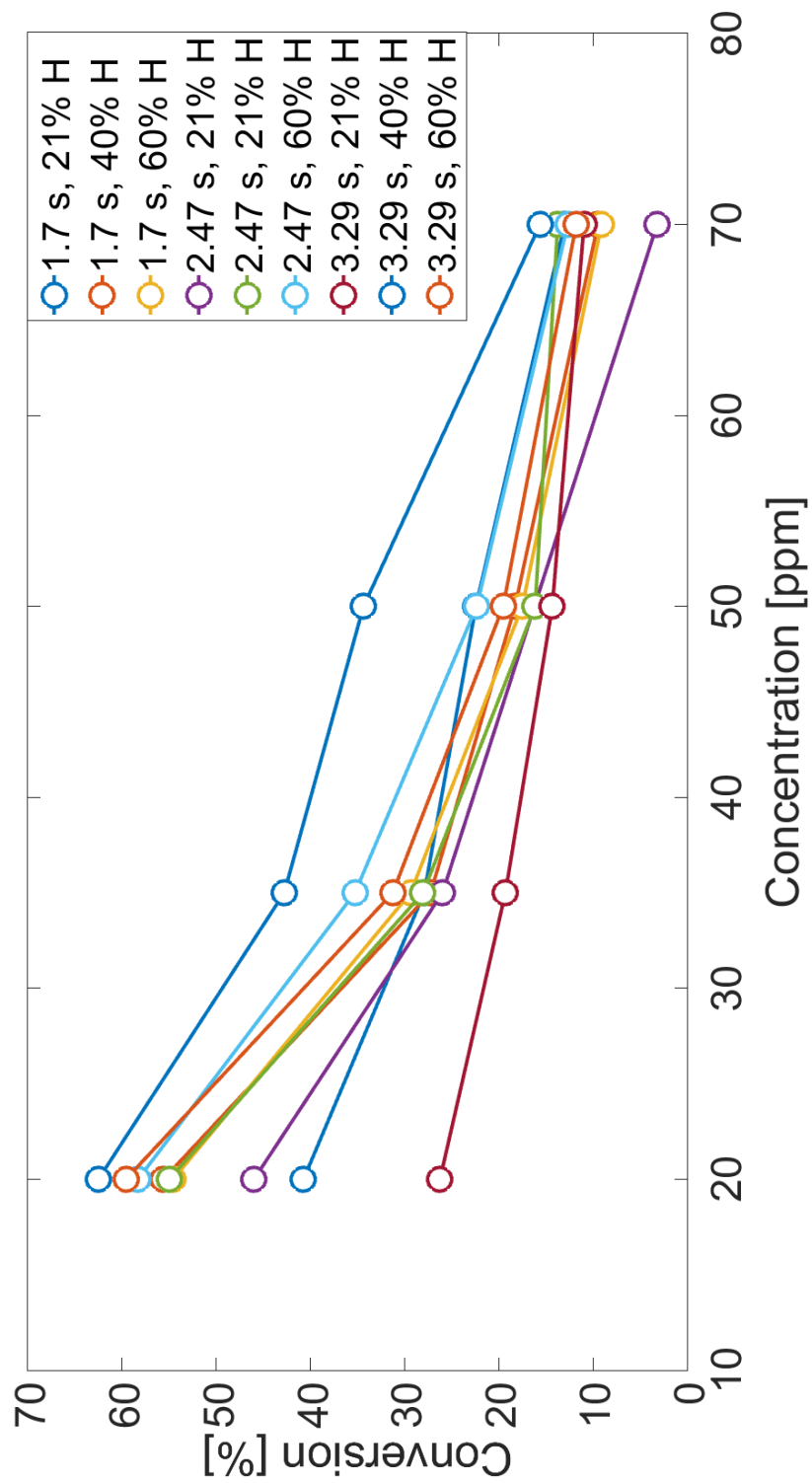


Figure 6.10 – Comparison between the degradation obtained for different inlet concentrations, for all the tests conducted

6.2.4 3D MATLAB plots

In order to have a better visualization of the results, two tridimensional MATLAB plots were done, summarizing the data obtained.

The first one, 6.11, shows the distribution of the conversion obtained for crossed value of humidity and residence times. Data referred to 20 *ppm* inlet concentration were chosen, since this concentration is significative for odor removal purposes and since the data obtained for this concentration are those that present the bigger sensibility to changes in main parameters, as seen in Figure 6.10.

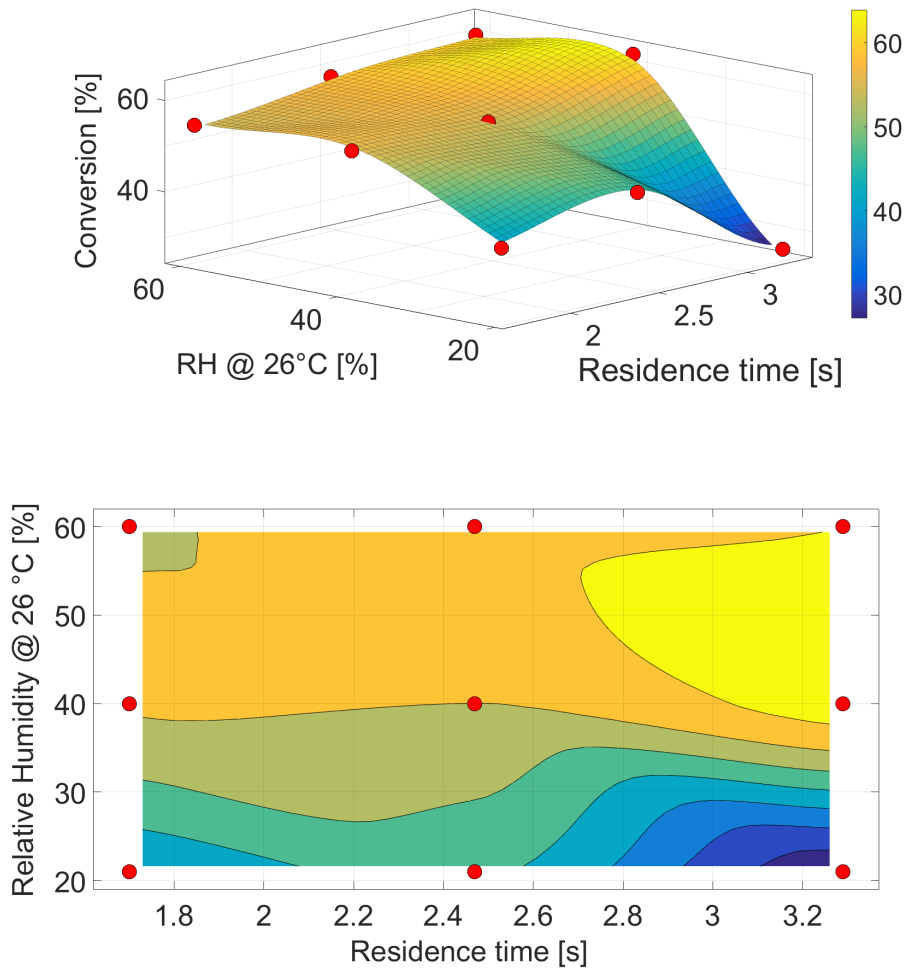


Figure 6.11 – Tridimensional visualization of the data obtained, showing the relation between conversion, flow rate (residence time), and humidity having 20 *ppm* as inlet concentration. Under the tridimensional graph, the corresponding contouring graph

The second diagram, 6.12, shows the outlet residual ozone measured for crossed value of RH and residence time. Since it was observed that the residual ozone was not significantly affected by the inlet concentration but just by humidity and residence time, the diagram shows the average residual ozone detected for the different inlet concentration, for both fixed humidity and flow rate.

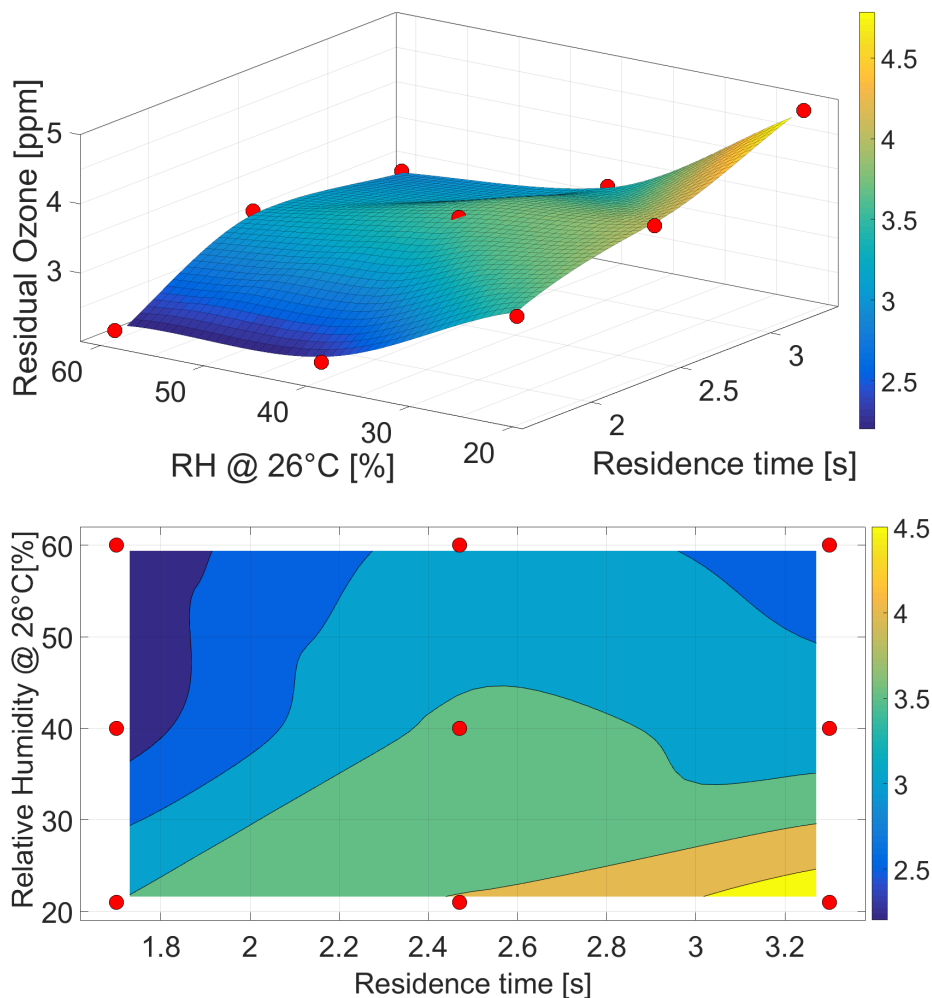


Figure 6.12 – Tridimensional visualization of the data obtained, showing the relation between average residual ozone, flow rate (residence time), and humidity. Under the tridimensional graph, the corresponding contouring graph

In order to obtain reference data about the behaviour of the ozone production/destruction, besides its reaction with Hydrogen sulfide, an additional series of experiments was conducted. This experiments consisted in a series of blank tests, with different humidity contents and residence times in the reactor, with the UV lamp switched on. No hydrogen sulfide was added. The summary of the results obtained from these tests is visible in the tridimensional plot 6.13.

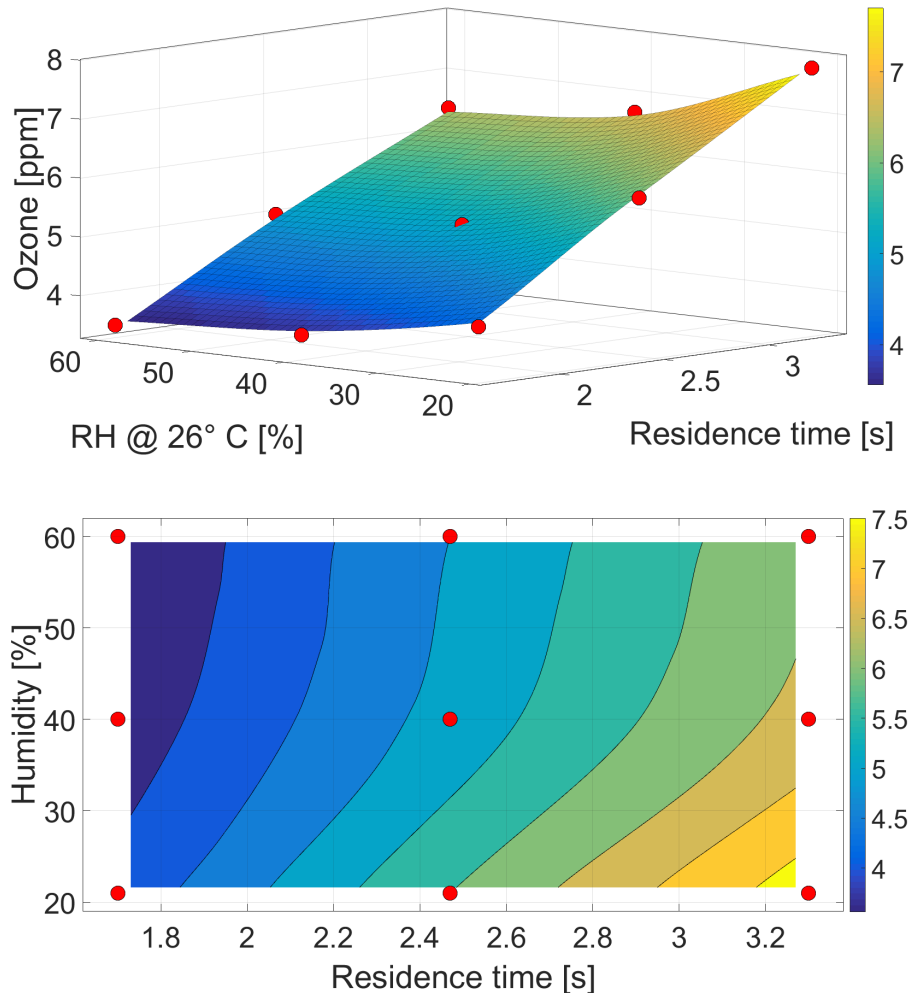


Figure 6.13 – Tridimensional visualization of the data obtained, showing the relation between residual ozone in blank tests, flow rate (residence time), and humidity. Under the tridimensional graph, the corresponding contouring graph

6.2.4.1 Analysis and discussion

The analysis of the data was conducted through a parallel comparison, zone by zone, of the tridimensional plot obtained for the conversion, 6.11, and the one obtained for the residual ozone, 6.12.

The first image, 6.14, shows the diagram zones belonging to low flow rates, 15 *l/min* (3.29 s of residence time). Looking at the figure, it is immediately possible to see a correspondence between conversion and ozone consumption: for high residence time and low humidity the conversion is lower and the ozone is higher, if compared to

the results obtained for similar conditions of residence time but higher humidity. In effect, for high residence time and high humidity content the conversion increases and the residual ozone decreases respectively. The best explanation for this trend is that the increase of conversion is due to the higher humidity content that enhances the production of OH radicals (reaction 3.5 and 3.3). The reaction of H_2S with OH radicals is known to be faster than the one with O_3 or UV light [14].

The production of OH radicals does not increase with the water content from 40% RH to 60% probably due to a competitive phenomena that occurs when the humidity content exceeds a certain level. The reactions that are possibly involved (3.10 to 3.13) are described in Section 3.

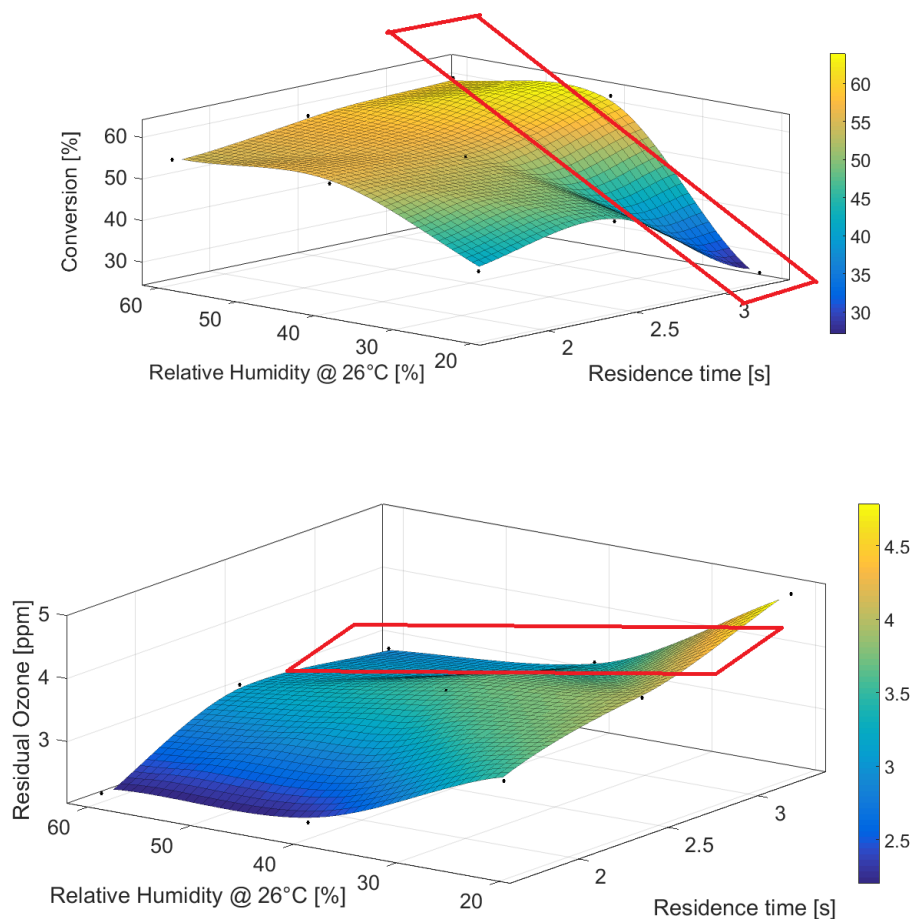


Figure 6.14 – Tridimensional visualization of the data obtained, showing the trend of two important parameters, residual ozone and conversion, in the graph area corresponding to high residence time (3.29 s)

The second image, 6.15, focuses on the charts area corresponding to low level of humidity. In this area the prevalent conversion mechanism is due to direct photolysis by the UV light and the presence of ozone, since the humidity is relatively low and so the formation of OH radicals.

In the conversion diagram it is possible to see an up/down trend with an initial increasing of the conversion with decreasing residence time followed by the subsequent decrease. On the other hand, on the same line, the ozone follows a continuous decreasing trend.

The possible explanation can be reduced to the formation of ozone inside the reactor. In fact this phenomenon occurs in the region just around the lamp so, the not sufficient mixing, corresponding to a low flow rate, cannot distribute properly the ozone inside the reactor, despite the higher residence time. This theory can explain the increasing degradation of hydrogen sulfide when the flow rate passed from 15 *l/min* (residence time of 3.29 s) to 20 *l/min* (residence time of 2.47 s). Although this hypothesis needs further investigations.

For what concerns the slightly decreasing degradation, that can be observed for 30 *l/min* of flow rate (residence time of 1.7 s) , it can be explained in terms of residence time: despite the higher mixing, the residence time is too short making some competitive reactions, that contribute to the O₃-consumption, prevail.

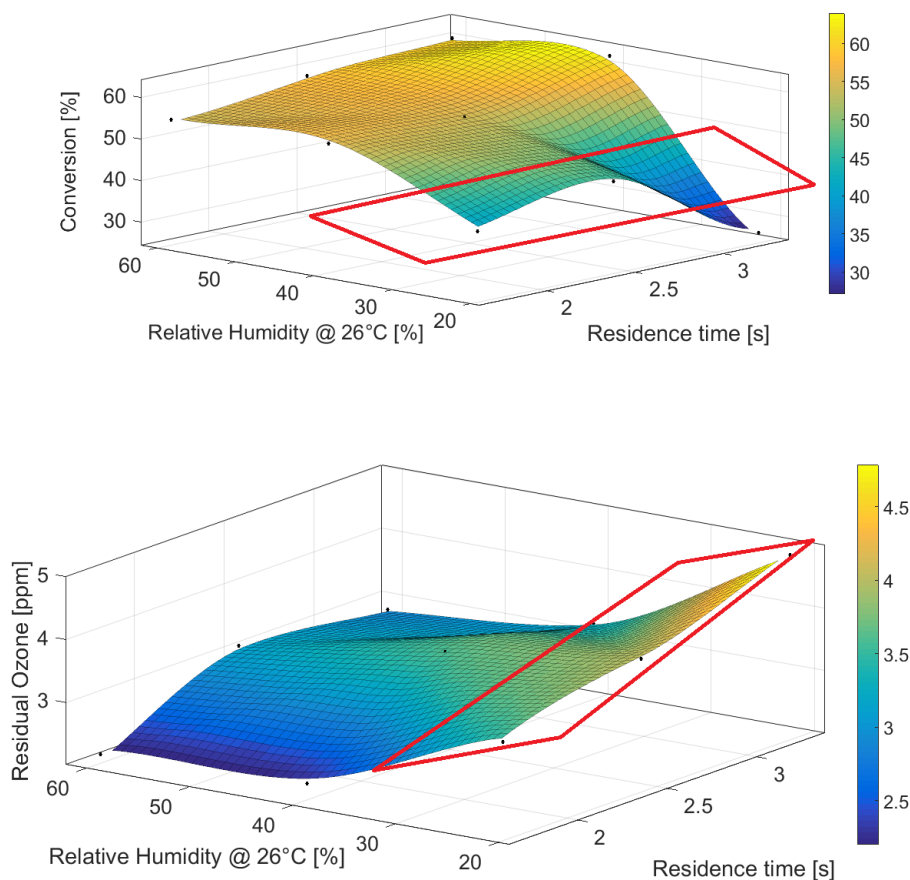


Figure 6.15 – Tridimensional visualization of the data obtained, showing the trend of two important parameters, residual ozone and conversion, in the graph area corresponding to low humidity

The third figure, 6.16, focuses on the diagrams region corresponding to high humidity levels and a residence time of 1.7 s. The diagram shows that the residual ozone decreases with increasing humidity and decreasing residence time, while the conversion has a plateau. Therefore the average value of conversion is higher if compared with those relative to low humidity conditions.

The conversion is lower if compared with the one obtained for higher residence times: this is probably because of the shorter residence time inside the reactor, despite of the same humidity conditions. The remarkable reduction of ozone corresponding to increasing flow rate, can be explained basing on a phenomenon of dilution, since the amount of ozone produced by the lamp per unit of time remains almost constant.

While, the reduction of ozone corresponding to increasing RH, is even due to the reaction of ozone with water for the formation of OH radicals and for competitive reactions.

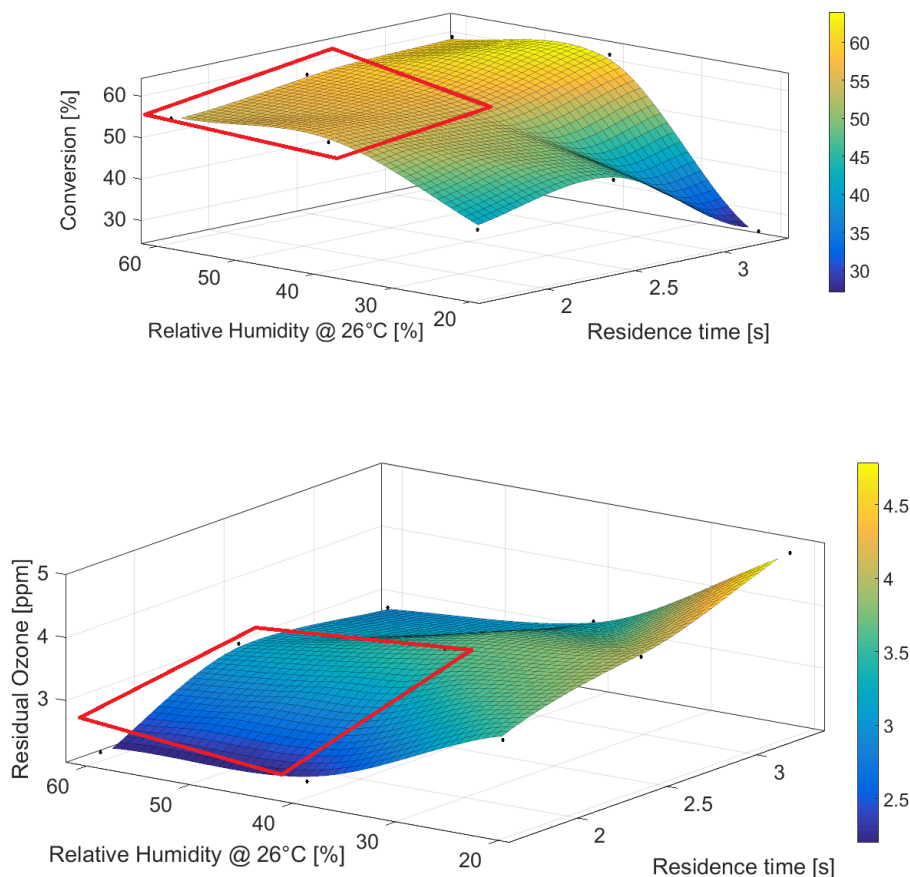


Figure 6.16 – Tridimensional visualization of the data obtained, showing the trend of two important parameters, residual ozone and conversion, in the graph area corresponding to high humidity and low residence time

In order to have a better visualization of the effective ozone consumption, a further tridimensional plot with MATLAB was obtained, by computing the difference between the data referring to the ozone blank tests and those referring to the residual ozone observed during the tests with addition of hydrogen sulfide.

The results obtained should give a qualitative idea of the ozone consumption due to : the formation of OH radicals, rection 3.3, the direct reaction with hydrogen sulfide3.8 and the contribution of the competitive scavenging reactions 3.10 3.11. The

competitive phenomena are most likely involved where, for same RH and residence time conditions, a high difference between data referring to the ozone blank tests and those referring to the residual ozone, does not correspond to an increased conversion. This happens in the area corresponding to high RH and high residence time, shown in figure 6.17.

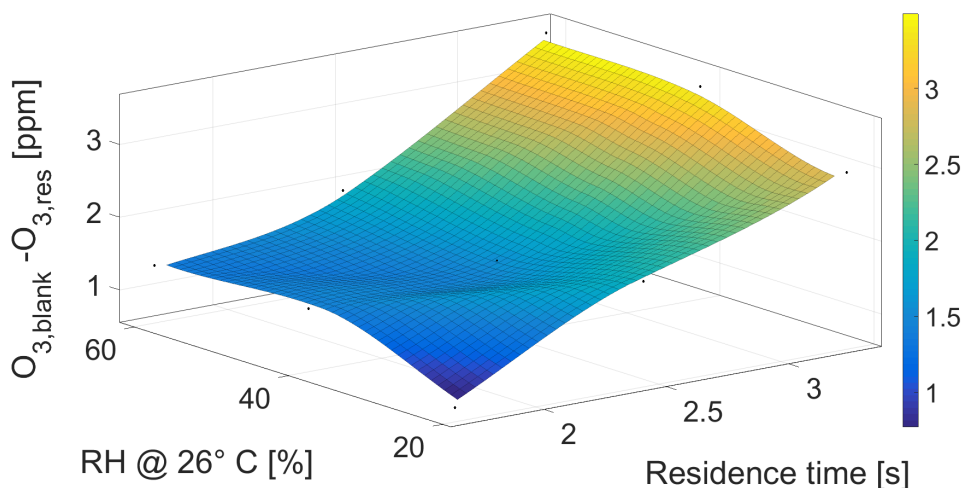


Figure 6.17 – Tridimensional visualization of the data obtained, the difference computed between the ozone detected in the blank tests and the residual ozone in the tests with addition on hydrogen sulfide

In order to evaluate the different mixing inside the reactor, two Computational Fluid Dynamics (CFD) simulation were conducted. The results are shown in figure 6.18. As is it possible to see, a slight difference in terms of velocity magnitude (m/s), does exist among the mixing in the reactor with a flow rate of 15 l/min (residence time of 3.49 s) and of 30 l/min (residence time of 1.7 s).

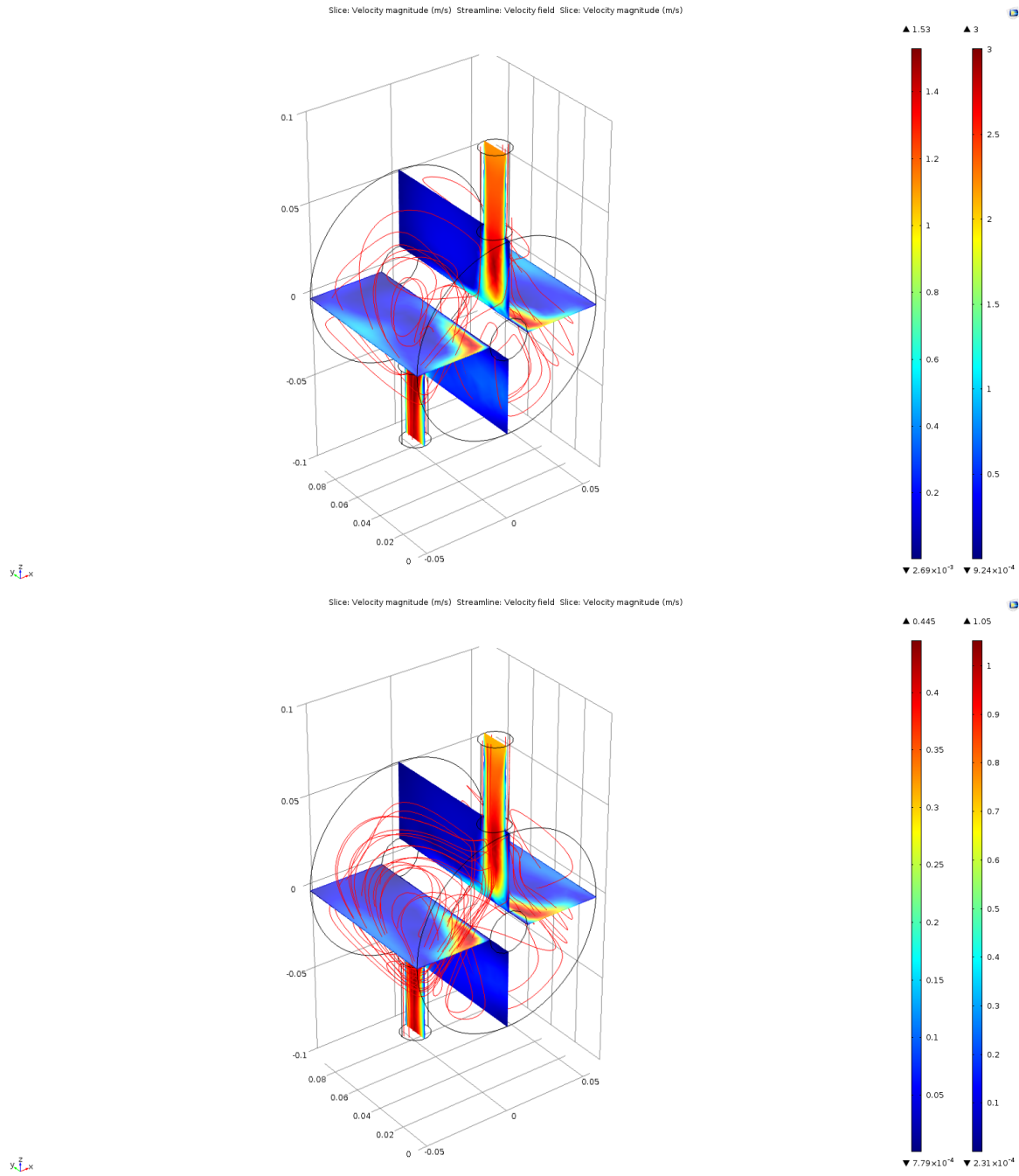


Figure 6.18 – CFD simulations (by Francesco Montecchio) showing the mixing inside the reactor. The the top one shows the mixing corresponding to 15 *l/min*. The bottom one shows the mixing corresponding to 30 *l/min*

Chapter 7

Conclusions

This study was conducted in order to evaluate the use of UV light technology in the field of hydrogen sulfide odour abatements treatments , with the aim to be less fuel consuming and subproducts producing (process water, sludge, adsorbent bed,...) if compared with the current technologies available. The results obtained show how this kind of technology could be suitable for the treatment of low concentration of this gas. In fact, for the condition that better mirrors the real industrial ones, low residence time (1.7 s) , the best degradation obtained was 55.61 % for 20 ppm fed into the reactor.

The immediate conclusion that can be inferred from these results is that this kind of technology requires a pre-treatment in order to be effective in the odour abatement processes. The other option could be its usage as a desulfurization unit as a first stage before other stages in the gas stream treatment, like activated carbon columns.

An exemplificative pre-treatment is proposed in the Appendix [A](#).

For what concerns the analysis of the influence of the main process parameters, the considerations that can be drawn are:

- The effect of humidity is more relevant for high residence times. From the graphs [6.14](#) the relation is quite evident, since the more humidity corresponds to the more degradation due to the more ozone consumption for the formation of OH^\bullet (see chapter [3](#)).
- For decreasing residence times, so in conditions more similar to the real cases,

Table 7.1 – Converison corresponding to different inlet concentration for a residence time of 1.7 s and different humidity contents

Inlet concentration [ppm]	$X_{\text{H}_2\text{S}}$ for 21% RH [%]	$X_{\text{H}_2\text{S}}$ for 40% RH [%]	$X_{\text{H}_2\text{S}}$ for 60% RH [%]
20	40.73	55.61	54.58
35	27.91	27.23	29.36
50	22.43	18.27	17.50
70	13.00	9.47	9.08

the more humidity does not corresponds necessary in an improvement of the effectiveness of the treatment. Despite the most common hypotesis[2], usually applicable to the VOC degradation using UV system [21], a high humidity level is not significantly affecting the conversion.

This is confirmed by the data obtained, that show that increasing humidity plays a beneficial role until it reaches the 40%. After this value, an additional increase of the water vapour does not affect the removal effectiveness of hydrogen sulfide, has a plateau. The possible explanation can be found in the phenomena described in chapter 3.

On the other end, additional humidity can be seen as a positive parameter since it contributes to reduce the residual ozone after the reactor. The ozone, that is not used in the conversion of hydrogen sulfide, through the formation of radicals, is consumed (see chapter 3) . This can be an useful information, since O_3 is usually cause of concern because of its toxicity (STEL for O_3 is 0.2 ppm) and because the abatement technologies for its removal are often expensive (i.e. catalytic supports).

- The mxing plays a fundamental role, since it enhances the collisions between molecules, improving the effectiveness of the treatment. However, further studies

are needed in order to investigate the magnitude of this influence and its limits.

- Inlet concentration influences the conversion rate, since a higher inlet concentration fed into the reactor corresponds to a decrease of the effectiveness of the treatment. The best conversion was observed for 20 ppm fed into the reactor. Moreover, for low concentrations, the process parameters such as RH and residence time, have a stronger influence on the conversion rate, compared to the one observed for higher concentrations. Moreover

Chapter 8

Future work

As preliminary study of the effectiveness of UV technology in the field of the odour emissions treatments, this Thesis provided results about the main process parameters. However in order to have a confirmation of its applicability in real cases, further investigations are needed to study it in a more heterogeneous and complex context. In particular, one of the aspects that have to be deepened, is the influence of a mixture of gases on the effectiveness of the UV technology. The gas more suitable for this study and their fractions, should be those that are usually present with Hydrogen sulfide in the different industrial context that has to be analyzed. The most common situations are summarized in table 8.1.

Another important aspect to be further analyzed is a detailed reaction mechanism coupled with a kinetic model. This kinetic study could help to determine which reaction prevails with certain conditions, making possible to manage and control better the overall process. The research of the best conditions conducted in this sense, could help to save resource in term of energy and materials.

For the same reason, one other future development could be targeted study of the relation between mixing inside the reactor and effectiveness of UV technology. This could be done through custom made reactors with an internal structure that can produce turbulent state.

A further investigations should be focused on the ozone formation mechanism by the UV lamp. This could help to confirm or refute the theory of the produced ozone

distribution around the lamp itself. One last future development could be the construction of a lab test rig including a pre- and after-treatment stage. All these developments could contribute to have the necessary parameters to make a cost/benefits analysis, useful for the construction of a pilot scale process unit.

Table 8.1 – Typical values of malodorous gases in different industrial plants

	H_2S [ppm]	Me_2S [ppm]	Me_2S_2 [ppm]	MeSH [ppm]	CS_2 [ppm]
Sludge decomposition facilities	-	Up to 10	Up to 10	-	-
Compost used as mushrooms [25] substrate cultivation	0.42	-	2.53	0.33	1.85
Aerobic composting of biowaste	-	-	Up to 10	-	-
Viscose rayon manufacturing	20 to 1000	-	-	-	20 to 1000
Kraft paper production	-	16.6	21.7	94	-

Bibliography

- [1] Energie- en milieu-informatiesysteem voor het vlaamse gewest, 2015.
- [2] Ryo Ono, Yusuke Nakagawa, Yusuke Tokumitsu, Hiroyuki Matsumoto, and Tet-suji Oda. Effect of humidity on the production of ozone and other radicals by low-pressure mercury lamps. *Journal of Photochemistry and Photobiology A: Chemistry*, 274:13 – 19, 2014.
- [3] Dräger’s guide to portable gas detection, 2012.
- [4] Agilent technologies website, 2015.
- [5] Roth S. H. Reiddenstein j.Hulbert C. Toxicology of hydrogen-sulfide. *Annual Rewiev of Pharmacology and Toxicology*, 32:109–134, 2002.
- [6] E. Smet, P. Lens, and H. Van Langenhove. Treatment of waste gases contaminated with odorous sulfur compounds. *Critical Reviews in Environmental Science and Technology*, 28(1):89–117, 1998.
- [7] E. Smet and H. Van Langenhove. Abatement of volatile organic sulfur compounds in odorous emissions from the bio-industry. *Biodegradation*, 9(3-4):273–284, 1998.
- [8] Christian Kennes and Frederic Thalasso. Review: Waste gas biotreatment technology. *Journal of Chemical Technology and Biotechnology*, 72(4):303–319, 1998.
- [9] Julia S. Kimbell Frederic J.-M. Moulin¹, Karrie A. Brenneman and David C. Dorman. Predicted regional flux of hydrogen sulfide correlates with distribution of nasal olfactory lesions in rats. *Oxford Journals, Toxicological Sciences*, 66(7-15):7–15, 2001.

- [10] David C. Dorman, Frederic J.-M. Moulin, Brian E. McManus, Kristen C. Mahle, R. Arden James, and Melanie F. Struve. Cytochrome oxidase inhibition induced by acute hydrogen sulfide inhalation: Correlation with tissue sulfide concentrations in the rat brain, liver, lung, and nasal epithelium. *Toxicological Sciences*, 65(1):18–25, 2002.
- [11] Gregory Leonardos, David Kendall, and Nancy Barnard. Odor threshold determinations of 53 odorant chemicals. *Journal of the Air Pollution Control Association*, 19(2):91–95, 1969.
- [12] C. Kennes and M.C. Veiga. Technologies for the abatement of odours and volatile organic and inorganic compounds. *Chemical Engineering Transactions*, 23:1–6, 2010. cited By 0.
- [13] K Mahmood A Turk and J Mozaffari. Activated carbon for air purification in new york city’s sewage treatment plants. *Water Science & Technology*, 27.
- [14] Jianhui Xu, Chaolin Li, Peng Liu, Di He, Jianfeng Wang, and Qian Zhang. Photolysis of low concentration {H₂S} under uv/vuv irradiation emitted from high frequency discharge electrodeless lamps. *Chemosphere*, 109:202 – 207, 2014.
- [15] Maria C. Canela, Rosana M. Alberici, and Wilson F. Jardim. Gas-phase destruction of {H₂S} using tio₂/uv-vis. *Journal of Photochemistry and Photobiology A: Chemistry*, 112(1):73 – 80, 1998.
- [16] Madhumita Bhowmick Ray. Photodegradation of the volatile organic compounds in the gas phase: A review. *Developments in Chemical Engineering and Mineral Processing*, 8(5-6):405–439, 2000.
- [17] Xiang Li, Guoqing Zhang, and Huageng Pan. Experimental study on ozone photolytic and photocatalytic degradation of {H₂S} using continuous flow mode. *Journal of Hazardous Materials*, 199 - 200:255 – 261, 2012.
- [18] R.H. Perry and D.W. Green. *Perry’s Chemical Engineers’ Handbook, 8th Edition*. McGraw-Hill, 2007.

- [19] V. Belgiorno, V. Naddeo, and T. Zarra. *Odour Impact Assessment Handbook*. Wiley, 2012.
- [20] Henry Persson. Photocatalytic oxidation for voc abatement, 2015.
- [21] Kuo-Pin Yu and Grace W.M. Lee. Decomposition of gas-phase toluene by the combination of ozone and photocatalytic oxidation process (TiO_2/uv , $\text{TiO}_2/\text{uv}/\text{O}_3$, and uv/O_3). *Applied Catalysis B: Environmental*, 75(1&2):29–38, 2007.
- [22] Yu Gang Chen Qing Zhu Wanpeng Zhang Pengyi, Liang Fuyan.
- [23] S. Popiel, Z. Witkiewicz, and M. Chrzanowski. Sulfur mustard destruction using ozone, uv, hydrogen peroxide and their combination. *Journal of Hazardous Materials*, 153(1-2):37–43, 2008. cited By 11.
- [24] Ozone monitor 2b technologies, inc, operation manual. models 106-l and 106-oem-l., 2014.
- [25] Van der Drift C Van Griensven LJLD Vogels GD Derikx PJJ, Op Den Camp HJM. Odorous sulfur compounds emitted during production of compost used as a substrate in mushroom cultivation. *Applied and Environmental Microbiology*, 1(56):176–180, 1990.

Appendix A

Study of a pre-treatment

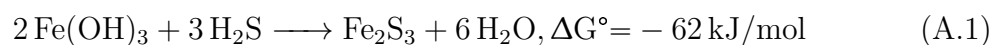
A deeper study on a pre-treatment stage for the abatement of H₂S was investigated, since the results obtained from the study conducted on the UV system show that this technology is reasonably effective only for concentrations lower than 30-35 ppm. For this purpose a chemisorption step was chosen as pretreatment to be investigated in this section.

A.1 Description of the material

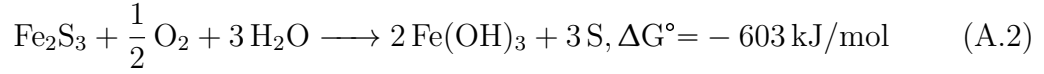
The absorbent beds used for this study was composed by granular ferric oxide/hydroxide. The commercial name is FerroSorp[®] S 2–4 mm(k).

FerroSorp[®] S appears like pelletised substance with a red brown colour, that is used for the desulphurisation of gases and air. The active element in the chemical composition is Ferric Hydroxide and its chemical formula is FeO(OH). The Fe content (Fe³⁺) is approx. the 20%, relating to the total solids amount.

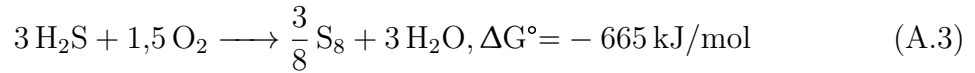
The removal of H₂S through the use of the FerroSorp[®] S can be described through the following chemical reactions:



Regeneration:



The following summary is a presentation of the overall process:



The reactions [A.1](#) and [A.2](#) are exothermic reactions whereby the regeneration reaction [A.2](#) creates a 10 times greater amount of heat than the absorption reaction.

A.2 Main parameters

The information to characterize the material were both provided by the supplier company, HeGo[®] Biotec, and partly integrated/confirmed through a BET characterization. The results obtained are shown in the in the figure [A.1](#).

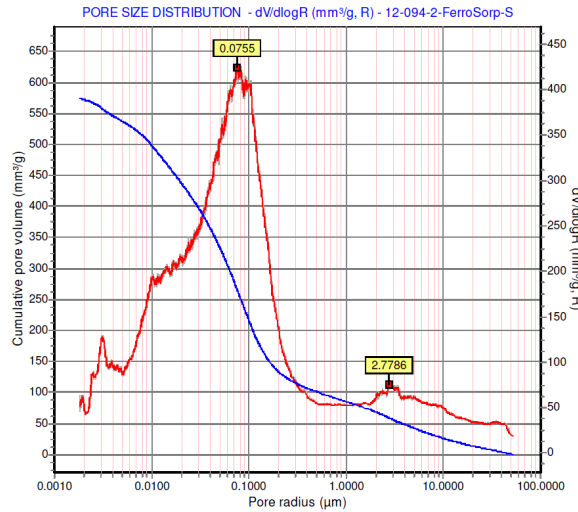


Figure A.1 – Pore size distribution of the granular ferric hydroxide provided by HeGo[®] Biotec

A.3 Methodology

Two beds were sized. The first one using the suggestions provided by the company: *EBCT* (Empty Bed Contact Time) corresponding to a minimum of 10 *s* and a maximum velocity of 10 *m/min*. Using these two parameters and considering a flow rate of 30 *l/min*, the total volume of the bed resulted 5 *l*. The internal diameter was fixed at 0.095 *m* and so the height resulted 0.071 *m*. In this first bed a gas stream with a concentration of 100 *ppm* was injected.

The second bed was sized to push as much as possible breakthrough time, in order to minimize the experiment time. For this reason the EBCT was fixed at 4.2 *s* with a resulting volume of 2.1 *l* and a bed height of 0.03 *m*. In this second bed a gas stream with a concentration of Hydrogen Sulfide of 150 *ppm* was injected. Figure A.2 shows the system configuration adopted.

A.4 System configuration: adsorption

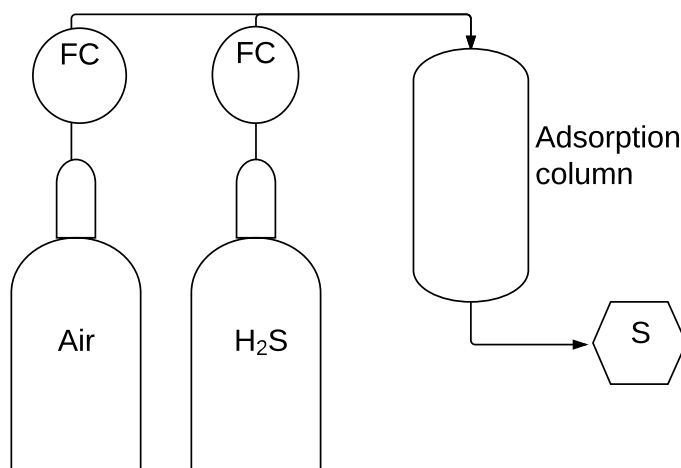


Figure A.2 – System scheme of adsorption with Iron Hydroxide

Since both the adsorption and the regeneration processes of FerroSorp[®] are exothermic reactions, the temperature of both beds was monitored in order to keep it under

60 °C. For this purpose a thermocouple was put in the middle of the beds. It is important to underline that during all the reaction time, no cooling was needed.

The graph A.3 shows the results obtained after several hours of exposition (2 to 20) of the filters to the contaminated gas stream. The two trend lines show the limit of the two beds to be used as pre-treatment before UV lamps.

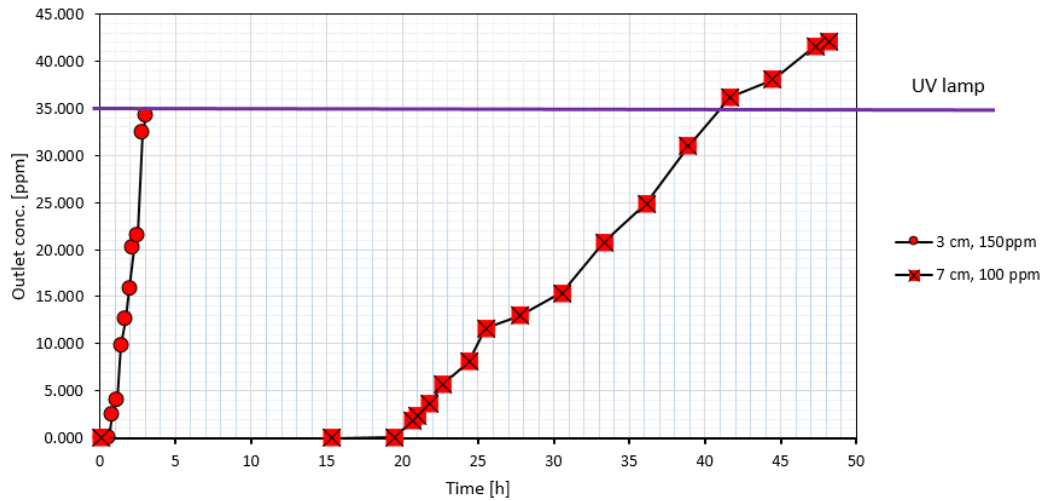


Figure A.3 – Outlet concentration from the pre-treatment beds VS time.

